Research Square

Preprints are preliminary reports that have not undergone peer review.
They should not be considered conclusive, used to inform clinical practice,
or referenced by the media as validated information.

NLRP3 Inflammasome Activation Dynamics are Shaped by Age, HIV-infection and Co- morbid Conditions

Shanshan Du
Yale School of Medicine
Archit Kumar
Yale School of Medicine
Bill Lee
Yale School of Medicine
Allen Esterly
Yale School of Medicine
Christopher Radcliffe
Yale School of Medicine
Lydia Barakat
Yale School of Medicine
Sui Tsang
Yale University
Allison Nelson
Yale School of Medicine
Iren Matos
Yale School of Medicine
Brent Vander Wyk
Yale University
Albert Shaw
Yale School of Medicine
Heidi Zapata
heidi.zapata@yale.edu
Yale School of Medicine

Research Article

Keywords:

Posted Date: November 18th, 2026

DOI: https://doi.org/10.21203/rs.3.rs-11614175/v1

License: This work is licensed under a Creative Commons Attribution 4.0 International License.
Read Full License

Additional Declarations: No competing interests reported.

Summary

Aging and chronic HIV infection are both associated with increased systemic inflammation, and people living with HIV-infection (PLH) have an increased risk of age-related diseases often occurring a decade before uninfected controls. The NLRP3 inflammasome is an intracellular sensor that has been implicated in age-related diseases. However, the combined effects of aging, HIV, and co-morbidities on inflammasome activation remain poorly defined. Here, we investigated NLRP3 inflammasome activity in white blood cells from adult cohorts stratified by HIV status, age, and comorbidity burden. We show that inflammasome activation is increased at baseline and dampened after stimulation in cells from older adults with increased co-morbid conditions, and in aging PLH. Gene expression analysis of purified monocytes showed increased IFN signaling at baseline with aging and HIV-infection. With stimulation we see an enrichment of neuronal receptors, and neuronal system pathways in older adults with increased co-morbidities, and a downregulation of TLR4 signaling in aging PLH. These findings demonstrate that increased age, HIV-infection and co-morbid conditions reshape inflammasome function.

NLRP3 Inflammasome Activation Dynamics are Shaped by Age, HIV-infection and Co-morbid Conditions

Shanshan Du[1]*, Archit Kumar[1]*, Bill Lee[1], Allen Esterly [1], Christopher Radcliffe[1], Lydia Barakat [3], Sui Tsang[2], Allison Nelson[1], Irene Matos[1], Brent Vander Wyk[2], Albert C Shaw[1], and Heidi J Zapata[1]

[1] Yale School of Medicine, Section of Infectious Diseases, Department of Internal Medicine, New Haven CT, [2] Yale University Program on Aging, [3] Yale University, Yale AIDS Care Program, New Haven, CT.

Corresponding Author: Heidi J Zapata: PO Box 208022, 300 Cedar street, New Haven, CT, 06520-8022. Fax number: 203-785-3864, Phone Number: 203-737-3659, heidi.zapata@yale.edu

*Both contributed equally to this manuscript and are first authors.

Abstract

With the advent of effective antiretroviral therapy, increased rates of age-related diseases such as cardiovascular disease and diabetes have been observed in people living with HIV (PLH). Persistent immune activation in PLH and age-related chronic inflammation are hypothesized to be drivers for the development of such diseases. Dysregulated NLRP3 inflammasome activation has been implicated in aging-related pathologies, but the combined impact of HIV and aging on inflammasome regulation remains poorly defined. To investigate this interplay, we enrolled a total of 147 subjects stratified by HIV status (positive/negative) and age. We found that older adults with increased co-morbidities and aging PLH had increased inflammasome activation at

baseline in monocytes compared to younger adults (demonstrated by elevated caspase-1 activation, elevated levels of IL-1β and IL-18), and a blunted response to microbial stimuli (LPS and LPS+ATP stimulation), with decreased production of IL-1β and IL-18. RNA-seq of purified monocytes revealed cohort-specific transcriptional programs associated with aging, HIV infection, and comorbidities both at baseline and with stimulation. The HIV-negative young cohort followed a predictable trajectory of inflammasome activation that was also mirrored in the transcriptional data of isolated monocytes where we saw an overall predictable increase in inflammasome gene expression. This coherence was lost in both older adults with higher comorbidity burden and aging PLH, who showed decoupling of RNA and protein with respect to inflammasome activation. Increased IFN signaling was noted at baseline in HIV-negative older adults and in aging PLH. With LPS stimulation, WGCNA analysis identified a gene module enriched for neuronal signaling and extracellular matrix remodeling that exhibited a stepwise increase in expression from HIV-negative young adults to subjects with increased age, HIV-infection, and greater comorbidity burden. HIV-positive older adults were noted to have downregulation of genes associated with TLR4 signaling. Collectively, our findings reveal that HIV, Aging and co-morbid conditions all reshape inflammasome dynamics—marked by baseline hyperactivation and blunted responsiveness to pathogenic stimuli.

Introduction

By 2030 it is estimated that 73% of people living with HIV (PLH) will be 50 years or older, with as many as 78% of such patients developing cardiovascular disease, 17% diabetes, and 17% malignancies[1]. It has been hypothesized that PLH have an accelerated form of aging manifested by an increased prevalence of age-related diseases, including cardiovascular disease, frailty, renal insufficiency, and bone loss, with many diseases occurring a decade

earlier than in HIV-negative individuals[2,3]. Chronic inflammation is often cited as an etiology for the increased risk of cardiovascular disease or other age related diseases in the setting of HIV-infection, although the mechanisms that link inflammation to this increased risk have not been fully elucidated [4]. Therefore, understanding the status of innate immune pathways at the convergence of aging and HIV-infection will be critical for determining whether targeting such inflammation can improve health outcomes in this growing population.

The NLRP3 inflammasome is a multiprotein complex that forms in response to stimulation of pattern recognition receptors by pathogen associated molecular patterns (PAMPs), such as LPS, or by Damage Associated Molecular Patterns (DAMPs). It is made up of the adaptor protein apoptosis-associated speck-like protein containing a CARD (ASC), and mediates the cleavage of pro-caspase-1 to activated caspase-1 and finally the cleavage of pro-IL-1β and pro-IL-18 to their active forms (IL-1β and IL-18) [5,6] . Classically, activation of the inflammasome requires a priming step (signal 1) that induces the TLR/NF-κB pathway and leads to increased expression of NLRP3/IL-1β, and a second step (signal 2), usually triggered by a PAMP/DAMP and leading to formation of the complex[5]. An alternative pathway of activation has been identified in human myeloid cells that can be triggered by lipopolysaccharide (LPS) alone[7,8]. Finally, inflammasome activation can trigger or be modulated by the expression of certain cytokines, including IL-6, TNF-α, IL-10 and IFN-β[9-12].

Dysregulation of the NLRP3 Inflammasome is strongly linked to the development of age-related diseases, including diabetes, and atherosclerosis[13-16]. In mice, the NLRP3 inflammasome has been shown to be essential for age-associated chronic inflammation; aged NLRP3 knockout mice showed extension of health span, with improved glycemic control and cognitive function, decreased bone loss and thymic involution when compared to aged wild-type mice[17]. While distinct mechanisms of NLRP3 inflammasome activation—including the

alternative pathway uniquely described in primary human monocytes[7]—have been well characterized, how these pathways are modulated by chronic disease and aging remains poorly understood. HIV infection and aging are both associated with systemic inflammation, a phenomenon often referred to as "inflammaging"[18-20]. However, it remains unclear how HIV infection and aging influence canonical versus alternative inflammasome activation in human monocytes. We hypothesize that these conditions remodel inflammasome signaling, contributing to dysregulated inflammatory responses in older adults, and aging PLH.

Increasing clinical evidence suggests that people living with HIV (PLH) exhibit heightened activation of the NLRP3 inflammasome. For example, higher plasma levels of IL-1β and IL-18 are associated with higher plaque scores and increased risk of cardiovascular events in PLH[21]. Increased levels of IL-1Ra (an IL-1 receptor antagonist) are noted in the plasma of HIV-infected individuals prior to a myocardial infarction[22], and autopsy-derived aortic plaques demonstrate higher levels of caspase-1[23]. At the cellular level, the NLRP3 inflammasome is known to be activated by components of HIV itself [24,25,26]. Chronic HIV-infection induces CD4+ T cell pyroptosis in an inflammasome-dependent manner (caspase-1 mediated)[27,28], and may thus contribute to systemic inflammation. However, significant knowledge gaps remain in understanding human NLRP3 inflammasome function at the interface of HIV and aging, particularly in innate immune cells. In this study we recruited young and older subjects with and without HIV-infection with the goal of evaluating inflammasome function in peripheral blood monocytes.

Results

Baseline caspase-1 activation in monocytes is elevated in the setting of increased age, HIV-infection and co-morbidities.

We recruited young (21-40) and older (>60 years), HIV-positive and HIV-negative subjects. Table 1 shows the breakdown of subjects used for this study. A total of 150 subjects was recruited for all of the studies. The cohorts included HIV-negative young adults (Young), HIV-positive young adults (HIV-Young), HIV-negative older adults (Older) and HIV-positive older adults (HIV-Older). Additionally, we recruited another group of HIV-negative older adults (Older*). This Older* group was initially recruited to better match co-morbid conditions such as smoking, alcohol and substance use disorders that were traditionally overrepresented in the HIV-positive older group. All HIV-positive subjects were on ART and had CD4+ counts >200/mm^3.

Freshly isolated PBMCs from all cohorts were used for downstream assays. We focused on evaluating monocytes which were subdivided into the following subsets, inflammatory ($CD14^+CD16^+$), classical ($CD14^+CD16^{lo}$), non-classical ($CD14^+CD16^H$), and activated monocytes ($CD11b^+CD14^+$)[29]. To begin, we assessed baseline caspase-1 activation using FAM-FLICA (FAM-YVAD-FMK) which contains a caspase-1 inhibitor (YVAD) sandwiched between a green, fluorescent label (carboxyfluorescein, FAM), providing a rapid and flexible method for analyzing active caspases[30]. We assessed baseline caspase-1 activation levels in activated ($CD11b^+CD14^+$) (Figure 1a), classical ($CD14^+CD16^{lo}$) (Figure 1b), inflammatory ($CD14^+CD16^+$) (Figure 1c), and non-classical ($CD14^+CD16^H$) (Figure 1d) monocytes. Baseline caspase-1 activity was elevated in the setting of HIV infection and in the Older* cohort. Increased caspase-1 activity was also noted in the HIV-Young cohort, compared to HIV-negative young adults. Across all four monocyte subsets, we observed a consistent trend:

baseline caspase-1 activity was significantly elevated in the HIV-positive young (HIV-Young), HIV-positive older (HIV-Older), and HIV-negative older (Older*) groups compared to the HIV-negative young group (Young), with the highest levels observed in the Older* group. No significant difference was observed between the HIV-negative young and the HIV-negative older group (Older).

Both HIV-positive and HIV-negative older adults exhibit a trend toward globally elevated cytokine levels at baseline when compared to HIV-negative young adults

Cytokine production in monocyte subsets was further analyzed across five cohorts at baseline using intracellular cytokine staining (ICS) and multicolor flow cytometry, with a focus on cleaved IL-1β (custom made antibody from Cell Signaling Technology (CST)), IL-18, IFN-β, IL-6, TNF-α, and IL-10 (Figure 1e and Supplementary Figures 1-3). Inflammasome activation is known to lead to increased production of IL-1β and IL-18. Inflammasome activation can also be modulated by or lead to the downstream induction of certain cytokines IL-6[9,31], TNF-α[10,32], IFN-β[12,33,34], and IL-10[11]. To enable cross-cohort comparisons of cytokine levels, a z-score transformation was applied, standardizing the cytokine values within each cohort to a mean of 0 and a standard deviation of 1. This normalization accounted for systematic differences between cohorts and facilitated the identification of cohort-specific cytokine patterns, independent of variations in absolute cytokine levels. The z-score analysis revealed distinct, cohort-specific cytokine profiles across monocyte subsets, and allowed a bird's eye view of cytokine profiles. The two young cohorts (HIV-negative and HIV-positive) collectively exhibited the lowest cytokine levels at baseline, forming a distinct cluster from older groups. In stark contrast, compared to the Young, both the HIV-positive older (HIV-Older) and HIV-negative Older*(Older*) cohorts showed a trend of a globally elevated inflammatory profile.

When we looked at individual cytokines and compared them between cohorts, we did not always see significant differences (Supplementary Figure 1-3) but saw some trends in increased cytokine levels in older adults. When we took an average of all cytokines ((TNF-α +IL-1β + IL-18 + IL-6 + IL-10 + IFN-β)/6) we did see a significant difference between the HIV-negative young cohort and both HIV-positive older and older* cohorts in inflammatory monocytes, and between HIV-negative young and HIV-positive older adults in activated monocytes (Supplementary Figure 9 a, c). Other comparisons were not significant. Overall, we saw a trend at baseline of the young cohorts exhibiting a decreased cytokine profile when compared to HIV-positive older adults and older* cohorts.

Older adults have an attenuated response to inflammasome activators (LPS and LPS+ ATP) when compared to young adults

We then set out to examine monocyte responses to LPS alone and LPS+ATP in the five cohorts using flow cytometry as noted above. As shown in Figure 2a-d, signal 1 (LPS alone) induced caspase-1 activation across all five cohorts, with a positive average percentage change in FAM-FLICA. No statistically significant differences were observed between cohorts in activated ($CD11b^{+}CD14^{+}$) or classical ($CD14^{+}CD16^{lo}$) monocytes-- exceptions were in inflammatory monocytes ($CD14^{+}CD16^{+}$) from HIV-Older individuals (HIV-Older) which exhibited reduced caspase-1 activation compared to the HIV-negative young (Young) cohort, and non-classical monocytes ($CD14^{+}CD16^{H}$) from the Older* cohort which displayed a significant increase following LPS stimulation when compared to the HIV-negative young (Young) cohort (Figure 2c-d).

With the addition of signal 2 (LPS+ATP), caspase-1 activation further increased across the Young cohort relative to LPS alone, although these changes did not always reach statistical significance across subsets. Responses in the Older, HIV-Older and Older* cohorts were mixed

across subsets. When comparing signal 2 to signal 1 within each cohort, a significant reduction in caspase-1 activation was observed in the activated and classical monocyte subsets among the Older, HIV-Older, and Older* groups (Figure 2a-b). In non-classical monocytes, however, following LPS + ATP stimulation, the Young, Older, and HIV-Older cohorts showed significantly enhanced caspase-1 activation compared to LPS alone (Figure 2d). In inflammatory monocytes, a significant reduction upon signal 2 was observed only showed in Older* group (Figure 2c).

With signal 2, the HIV-Young, Older and HIV-Older all showed significantly reduced caspase-1 activation compared to the Young cohort in activated, classical and non-classical monocytes (Figure 2a, b, d). The Older* cohort showed a significant decrease in caspase-1 activation in all monocyte subsets compared to the Young cohort (Figure 2 a-d). Overall, these findings show differential inflammasome responses to secondary stimuli across monocytes subsets, with aging and HIV-infected cohorts generally exhibiting attenuated caspase-1 activation, except for non-classical monocytes, where enhanced activation was observed.

We also evaluated cytokine production in response to LPS alone and LPS + ATP stimulation across the five cohorts (Figure 2e and Supplementary Figure 4-6). Radar plots (Figure 2e) illustrate the relative changes in six cytokines (IL-1β, IL-18, TNF-α, IL-6, IFN-β, and IL-10) across cohorts, normalized as z-scores. Upon LPS stimulation (Figure 2e), the Young cohort exhibited the most pronounced cytokine expression (as indicated in blue), with increased production of IL-1β and IL-18 compared to all other cohorts. Production of IL-1β and IL-18 decreased in the following order across monocyte subsets (excluding non-classical monocytes); HIV-negative young (Young), HIV-positive young (HIV-Young), HIV-negative Older (Older), HIV-positive Older (HIV-Older), HIV-negative Older* (Older*). The HIV-negative Older* cohort had the smallest area when compared to all other cohorts (as indicated in yellow). Supplementary

Figure 4-6 presents the absolute percentage changes with statistical comparisons. These results support the trend observed in the radar plots. These findings suggest that Inflammasome activation in response to LPS is impaired in the context of HIV infection, aging and comorbidities.

With the addition of signal two (ATP) we see that the HIV-negative young (Young) cohort continues to have the largest area (in blue) and maintains the production of IL-1β and IL-18 in the activated and classical monocytes subsets, whereas we see a decrease in area or no change in the HIV-positive young (HIV-Young), HIV-positive older (HIV-Older) and Older* cohort. If we follow the example of the activated and classical monocyte subsets, we see (Figure 2e and Supplementary Figure 4-6) that the HIV-negative young cohort has the largest production of IL-1β and IL-18, and it decreases in production in the following order: Young, HIV-Young, Older, HIV-Older, and Older*. Each cohort exhibited distinct cytokine patterns across specific monocyte subsets, highlighting differential immune regulation in response to LPS or LPS + ATP stimulation. While not all comparisons were statistically significant-- the results do support a general trend of attenuation.

Overall, we saw that HIV-negative young adults had the most robust production of IL-1β and IL-18 when compared to older adults with HIV-infection and the Older* cohort. Most of these comparisons were significant when we examined individual cytokines in activated, and classical monocytes (Supplementary Figure 4). When we took an average of all cytokines ((TNF-α +IL-1β + IL-18 + IL-6 + IL-10 + IFN-β)/6) we saw a significant attenuated response with increased age, HIV-infection and co-morbid conditions mostly in activated and classical monocytes (Supplementary Figure 10 a, c).

We also examined other cytokines that can be induced downstream of the inflammasome. A few individuals had increases in IL-10 with both LPS and LPS+ATP stimulation although the

differences were not significant. The only significant comparisons were seen with the older* cohort which had a significant decrease in TNF-α production when compared to other cohorts under both LPS and LPS+ATP stimulation conditions in most monocyte subsets. Regarding IL-6, the Older* cohort also demonstrated significantly lower production compared to the Young cohort in most monocyte subsets under LPS stimulation (Figure 2e, Supplementary Figure 6i-p). A trend of impaired cytokine production was also observed for IFN-β in the HIV-Older cohort when compared to other cohorts, though the comparisons were only significant in the activated monocyte subset.

Overall, we see that the HIV-negative young cohort follows a predictable course of decreased inflammation at baseline (decreased caspase-1 activation), and increased production of IL-1β, and IL-18 (along with increased Caspase-1) with stimulation. However, with HIV-positive older adults and the older* cohort we see evidence of increased inflammasome activation at baseline, with increased caspase-1 activation, and trends of increased cytokine levels at baseline. With stimulation these older groups show a dampened response to stimulation.

Clinical Data

Table 2 shows the distribution of sex, race and ethnicity among the cohorts. There were significant differences noted in race/ethnicity. Review of the clinical data showed that the older cohorts all had significantly increased co-morbid condition counts when compared to the young cohorts (Supplementary Figure 8). Additionally, the HIV-positive young cohort had increased co-morbid conditions when compared to the HIV-negative young cohort. There were no significant differences noted between the three older cohorts when co-morbid conditions were counted (Supplementary Figure 8). It is notable that the Older* cohort often had a distinct inflammatory signature when compared to other older cohorts. The Older* cohort was originally recruited to better match the increased frequency of smoking, alcohol and substance abuse

seen in the HIV-positive older group. Table 3 shows the frequencies of certain co-morbid clusters among the older cohorts. These were organized accordingly: **behavioral** (smoking, alcohol abuse, substance abuse), **metabolic** (obesity (BMI ≥ 30, diabetes, high cholesterol), **cardiovascular** (hypertension, coronary artery disease (CAD), myocardial infarction (MI), congestive heart failure (CHF), peripheral vascular disease (PVD), arrythmias, valvular disease), **pulmonary** (asthma, COPD, lung disease, sleep apnea), **inflammatory** (autoimmune, colitis, thyroid disease, osteoarthritis) and **organ disease** (kidney disease, liver disease).

Table 3 shows that rates of the behavioral cluster were similar in both the HIV-Older and Older * cohort, and show a trend of higher substance use compared to the HIV-negative older cohort (although the differences were not significant). When we further compared all three older cohorts (Table 3) we did see significant differences in race/ethnicity, and in the inflammatory and organ failure cluster. We saw trends of significance in gender. Females dominated in the Older* cohort (81.8%) compared to the other older cohorts (Table 3); biological sex has been shown to affect inflammasome activation[35]. The organ failure cluster (kidney disease and liver disease) dominated in the HIV-Older cohort and the inflammatory cluster (autoimmune disease, colitis, thyroid disease, osteoarthritis) dominated in the HIV-negative older cohort (Older). Finally, when the Older* cohort was compared to the other older cohorts in Table 4, we saw a significant increase in COPD, and a trend toward increased smoking, and osteoarthritis in the Older* cohort, suggesting these clinical variables could contribute to the biological differences associated with the Older * cohort.

Statistical Analysis of Cytokine Data with Linear Regression Modeling

We then proceeded with a progression of linear models that firstly included factors of age (older and younger) and HIV status (positive and negative) and adjusted for confounders (race/ethnicity and gender) (Table 2). In follow-up analyses, factors of age and HIV were exchanged for a single factor denoting cohort status [(HIV-negative Older (Older), HIV-positive older adults (HIV-Older), and Older*)]. In Figure 3, we explored the factors of age and HIV-infection. Results are presented for the main effect of age (reference group is younger) and HIV status (reference group is HIV negative). The main effects are depicted on the heatmaps of Figure 3 (panels a, c), and on the x-axis of the corresponding scatterplot (panels b, d). A positive main effect means that the comparison group shows a stronger response than the reference group (older > younger or HIV positive > HIV negative), while a negative main effect indicates the reverse (older < younger or HIV positive < HIV negative For example, a positive main effect of age is increased IL-18 expression at baseline in CD11b+, CD14+CD16+, and CD14+CD16lo monocytes. A positive main effect of HIV-infection was elevated IL-10 at baseline in CD14+CD16H monocytes. A negative main effect of age was decreased IL-18 production with LPS+ATP stimulation in classical monocytes. A negative main effect of HIV is decreased IFN-β production in classical or activated monocytes with LPS and LPS+ATP stimulation.

An interaction means that the effect of one dimension differs as function of the other dimension, i.e. the effect of age differs by HIV status. The interaction effect is depicted on the y-axis of each scatter plot (panels b, d) and gives the change in the main effect in the HIV Positive (b) or older (d) subgroup, with the HIV-negative or younger subgroup as the reference. We use the terms amplification, attenuation, and crossover to describe patterns of interaction. For example, a positive main effect of HIV status that is larger in older individuals would show up on the right side of the figure above the horizontal axis, and we refer to that as an amplification, if the effect was significant. An example of an amplification interaction would be increased IL-1β and IL-6

315 production in CD14+CD16H monocytes with LPS and LPS+ATP stimulation in HIV-Older adults
316 as noted by blue squares and triangles (Figure 3 d).
317
318 A positive main effect, that is instead smaller in older individuals would still be on the right side,
319 but would sit below the x-axis, and we would label that as an attenuation (if significant). An
320 example would be lower production of TNF-α in CD14+CD16+ monocytes with LPS+ATP
321 stimulation in HIV-positive older adults. A negative main effect of HIV (HIV positive < HIV
322 negative), would be on the left side of the plot, with amplification now being applied to points
323 below the x-axis, and attenuation to points above the x-axis. An example would be a decrease
324 in IFN-β production (green star) noted HIV-older subjects with LPS stimulation (Figure 3d). The
325 rationale in this case is that the positive effect of age (up on the y-axis) is attenuating the
326 negative main effect of HIV relative to the reference group. And correspondingly, a negative
327 effect of age (down on the y-axis) is amplifying the negative main effect of HIV relative to the
328 reference group (HIV-negative). Since the reference groups are arbitrary, it should be noted
329 that changing the reference group would flip the corresponding axis and change the label but
330 wouldn't change the effect or its significance.
331
332 Now if we look at a negative effect of age in Figure 3b that is higher in the HIV-positive such as
333 decreased production of IL-1β in CD14+CD16+ monocytes with LPS+ATP stimulation. We see
334 an attenuation of this effect in HIV-positive individuals with the cytokines IL-1β and IL-6 with
335 stimulation in non-classical monocytes (CD14+CD16H) (green symbols). Crossover effects
336 appear in the middle of the figure, above or below the x-axis. These represent patterns where
337 the effects for the subgroups are in opposite directions. And since the main effect is the average
338 of the effects in the subgroups, a crossover often occurs with no main effect (near 0 on the x-
339 axis). No significant cross over events were noted.

Overall, for markers that showed an age effect, HIV-infection tended to reduce the magnitude of this effect. And markers that showed an HIV effect, tended to be amplified by age.

Finally, the older cohorts' effects figure (Supplementary Figure 7) examines significant differences noted between the older cohorts. For the most part, the Older* differed from the other older cohorts. For example, the Older* cohort was noted to have increased TNF-α levels at baseline across all monocyte subsets(Supplementary Figure 7) when compared to both the HIV-Older cohort and the HIV-negative older cohort.

Older Adults with HIV-infection and co-morbid conditions show decoupling of Inflammasome related gene expression and protein expression during LPS stimulation

We proceeded with bulk RNA seq of purified monocytes to further elucidate the underlying mechanisms responsible for the cohort differences seen in inflammasome response. Monocytes were negatively selected from PBMCs and stimulated with LPS for 6 hours prior to RNA extraction. RNA was subsequently extracted for bulk RNA sequencing to assess transcriptional changes. Principal component analysis (PCA) revealed that PC1 and PC2 accounted for 72% of the total variance, clearly separating the baseline monocytes from LPS stimulation (Figure 4a). PC1, which captured the majority of the variance (65%), was strongly associated with LPS stimulation ($p = 1.13 \times 10^{-25}$). PC2, accounting for 7% of the variance, and PC5 (2.4%) were both significantly associated with cohort identity (PC2: $p = 3.21 \times 10^{-2}$); PC5: $p = 2.80 \times 10^{-3}$), indicating biologically meaningful variation beyond the global LPS response. To further characterize the biological processes driving each PC, pathway enrichment analysis was performed using iDEP 0.96[36], which ranks genes by their PCA loadings and tests for

overrepresentation in MSigDB Hallmark gene sets (Figure 4b). PC1 was enriched for inflammatory pathways, including TNFα signaling via NF-κB, inflammatory response, interferon-α, and interferon-γ responses, consistent with LPS-induced activation. In contrast, cohort associated PCs (PC2, and PC5) were enriched for DNA repair, the unfolded protein response (PC2), and cholesterol homeostasis (PC5), suggesting cohort-specific regulation of stress and metabolic pathways. PC3 and PC4 were not associated with cohort identity or stimulation.

Focusing on the HIV-negative young and older cohorts revealed distinct age-dependent clustering that emerged in the PCA. PC1 (62.2% variance) separated control and LPS-stimulated samples, delineating both young and older groups based on their LPS response. PC2 (6.9% variance) further separated the groups by age, highlighting distinct transcriptional profiles between Young and Older cohorts under both control and LPS stimulation (Figure 4c). Correlation analysis (Figure 4d) confirmed that PC1 was strongly associated with LPS stimulation, while PC2 was significantly associated with age. PC1 was enriched for inflammatory pathways such as TNF-α signaling, Interferon Responses, and separated LPS-stimulated from control samples in both Young and Older cohorts. Meanwhile, PC2 captured age-associated transcriptional differences (mTORC1, G2M checkpoint, Myc targets) which were evident in both control and LPS-stimulated samples (Figure 4d). PC3-5 were not associated with either age or stimulation. Overall, LPS stimulation led to the expected induction of inflammatory pathways that were expressed in both young and old, however we also saw that aging also triggered other cellular pathways involved in mTORC signaling, cell cycle progression, Myc targets, and estrogen signaling.

When we examine inflammasome specific genes in all cohorts we see that most genes show low baseline expression and appropriately increase with LPS stimulation (Figure 5). However, a subset of inflammasome genes shows high baseline expression and decrease upon LPS

388 stimulation. Notably, canonical, non-canonical, and alternative inflammasome pathways,
389 including *IL1B, NLRP3, CASP1, CASP4*, *CASP5, NFKB1, NFKB2, PANX1,* and *BCL2,* were
390 consistently upregulated across all cohorts upon LPS stimulation, whereas *CTSB*, *HMOX1*,
391 *NAIP*, *CASP8*, *PYCARD*, *NLRC4*, *NLRP1*, *NALP*, and *NOD2* showed consistent
392 downregulation. To validate the RNA-seq findings, we further performed RT-qPCR on purified
393 monocytes stimulated with LPS for 6 hours (Figure 5b-e). We assessed the expression of
394 representative genes involved in inflammasome signaling, including *IL1B* and *CASP1*, *CASP4*,
395 and *CASP5* (non-canonical pathway). Consistent with the transcriptomic data, *IL1B* was
396 significantly upregulated upon LPS stimulation in all cohorts, with significantly higher expression
397 noted in the HIV-negative young (Young) cohort when compared to the other cohorts. *CASP1*
398 expression also increased across all cohorts following LPS stimulation and showed a trend
399 towards decreased expression with increased age and HIV-infection. Both *CASP4* and *CASP5*
400 were also upregulated following LPS exposure, particularly in HIV-Young, Older, and HIV-Older
401 cohorts. Notably, *CASP5* expression was significantly higher in the Older* cohort compared to
402 the Young cohort. Interestingly, we saw that both the canonical (Caspase-1) and non-canonical
403 pathway (Caspase 4 and Caspase 5) were simultaneously induced in all cohorts.

404 Overall, the HIV-negative young cohort follows a predictable trajectory of inflammasome
405 activation. At baseline they exhibited low levels of caspase-1 activation and inflammatory
406 cytokines (IL-1β, IL-18 etc.). With LPS and LPS + ATP stimulation, they show an appropriate
407 increase in production of IL-β, and IL-18, and caspase-1 activation. This coordinated trajectory
408 in protein production was mirrored in the transcriptional data. Interestingly, this predictable
409 trajectory was disrupted in in older adults with HIV-infection and co-morbid conditions (HIV-
410 Older, and Older*). Specifically, we observed a decoupling at protein level, with elevated
411 inflammasome activation at baseline but an attenuated response to stimulation. A decoupling
412 of RNA and protein expression has been noted with aging in a number of studies[37,38]. It is

possible that post translational modifications are driving the differences we see across our cohorts[39].

Transcriptional Variation in Monocytes Across Age, HIV, and Comorbid Conditions

Despite a similar response in inflammasome gene expression, we then set out to delineate other remaining differences in gene expression across cohorts with LPS stimulation. Baseline differences in pathway activity across age and HIV status groups were first assessed using GSEA based on DESeq2-derived differential expression results. At baseline key hallmark inflammatory pathways, such as TNFα signaling via NF-κB and inflammatory response, had low expression in the HIV-Young, Older, and HIV-Older cohorts compared to the Young cohort at baseline. These pathways notably had increased expression in the Older* group relative to Older (Figure 6a). The Hallmark interferon gamma response and interferon alpha response was notably upregulated in the HIV-Older and Older* cohort when compared to both the young and older HIV-negative cohorts.

We then applied a linear model to compare LPS stimulation responses of monocytes across the five cohorts. The resulting ranked gene lists were subjected to GSEA analysis. First, we evaluated the comparison of the delta or change from baseline with LPS stimulation (e.g., Δ HIV-Older/Δ Young) between cohorts to identify pathways with differential LPS responsiveness across cohorts (Figure 6b); and second, we evaluated LPS vs control within each cohort to identify pathways activated by LPS in each cohort independently (Supplementary Figure 11c). Upon LPS stimulation, all cohorts exhibited upregulation of the Inflammatory response and TNFα signaling pathways, as well as Interferon gamma responses (Supplementary Figure 11c). Additionally, all cohorts except the Young group exhibited upregulation of IL-6 and IL-2 signaling which notably decreased in the older cohorts compared to the HIV-Young cohort (Supplementary Figure 11c). Compared to the Young group, HIV-positive young adults

displayed significantly enhanced LPS responses, with positive enrichment across all major immune-related pathways, including TNFα signaling via NF-κB, interferon α/γ responses, the inflammatory response, IL-6 and IL-2 signaling (Figure 6b). Similarly, the Older cohort showed stronger induction of interferon responses, inflammatory signaling, IL-6 and IL-2 signaling relative to Young (Figure 6b). In contrast, the HIV-Older cohort exhibited a more complex pattern. Although absolute expression of TNFα and inflammatory response genes was elevated (Supplementary Figure 11c), their dynamic responsiveness to LPS—particularly in the interferon pathways—was blunted compared to the Young cohort (Figure 6b). Likewise, the Older* cohort showed weaker responses than the Young cohort across most pathways, including interferon responses, inflammatory signaling, IL-6 signaling, TNFα signaling via NF-κB.

To complement the interaction analysis, we performed differential expression gene (DEG) analysis within each cohort independently, comparing LPS-stimulated versus baseline samples using DESeq2. The results are summarized in Supplementary Figure 11 (a and b), where UpSet plots illustrate the number of significantly upregulated and downregulated genes in each group, as well as their intersections across cohorts. The HIV-negative Older* cohort exhibited the most robust transcriptional activation, with 4,383 upregulated genes, including 2,552 uniquely upregulated genes. In contrast, the HIV negative young (Young) cohort displayed the highest number of significantly downregulated genes (1,438 genes). Across all five cohorts, 863 genes were commonly upregulated, and 660 genes were consistently downregulated, indicating both shared and cohort-specific transcriptional responses to LPS. To explore the functional implications of these cohort-specific responses, we conducted pathway enrichment analysis on the unique DEGs in each group (Figure 6 c, d). Unique genes were defined as those significantly up- or down-regulated in only one cohort and not differentially expressed in the

other four cohorts. Among uniquely upregulated genes, the Older* cohort was enriched in pathways related to neuronal signaling (e.g., neurotransmitter receptors and postsynaptic signaling, neuronal system), cell structure and matrix remodeling (e.g., degradation of extracellular matrix, collagen chain trimerization). Genes that were upregulated were multiple neuroreceptors such as *CNR1* (Cannaboid receptor 1), *GRM7* (Glutamate receptor 7), and *OPRM1* (Opioid receptor mu 1) and *ADCY2* (Adenylate Cyclase 2) (Supplementary Figure 12). The Young cohort showed specific upregulation of the hallmark G2M checkpoint, MYC targets v1, fatty acid metabolism, and allograft rejection pathways (Figure 6c). The HIV positive young group (HIV-Young) also shared upregulation of MYC targets v1 and allograft rejection, but also showed specific upregulation of the inflammatory response, PI3K–Akt–mTOR signaling, the unfolded protein response, and hallmark MYC targets v2. Although, the HIV-negative young and HIV-positive young cohort shared upregulation of the Hallmark Allograft rejection pathway—the underlying gene drivers were unique in each cohort. For cohort-specific downregulated genes (Figure 6d), the HIV-negative Older* group showed decreased activity in pathways including fatty acid metabolism, adipogenesis, complement cascade, and mTORC1 signaling. Notably, the HIV-Older cohort exhibited specific and significant downregulation of 66 genes. Pathway enrichment analysis revealed that several genes, *FADD*, *TICAM2*, *MAPK14*, *BTRC*, *GASDMD*, all are involved in the Toll-like receptor 4 (TLR4) signaling cascade. Taken together, these results highlight distinct, cohort-specific transcriptional programs activated or suppressed in response to LPS stimulation, reflecting both age- and HIV-associated alterations in immune and metabolic signaling pathways.

Gene Co-Expression Analysis Highlights Inflammaging Trajectories and Cohort-Specific Transcriptional Patterns

Given the pathway-level differences observed across cohorts, we next investigated whether coordinated transcriptional programs might underlie these changes. Weighted gene co-expression network analysis (WGCNA) was conducted on the top 2,996 most variable expressed genes across all samples (Figure 7a). We correlated the module eigengenes (the average expression pattern of each gene module) with cohort identity to identify gene networks associated with inflammation and clinical status. Particular attention was given to modules enriched for immune or inflammatory pathways that could reflect progressive immune activation across cohorts.

WGCNA identified four distinct gene modules: Brown (178 genes), Yellow (44 genes), Blue (853 genes), and Turquoise (1,921 genes), using a soft threshold power of 5 and a minimum module size of 20. Among the identified gene modules, the Blue module, comprising 853 genes, exhibited a significant stepwise increase in eigengene expression across cohorts under LPS stimulation, consistent with an amplified inflammatory transcriptional response (Figure 7b). Post-hoc analysis confirmed significant elevation in the Older* cohort compared to Young controls, demonstrating a cohort-dependent escalation of inflammatory transcriptional programs (Figure 7b, Supplementary Figure 13). To further characterize the internal structure of this module, a co-expression network was constructed (Figure 7c), with nodes representing genes and edges indicating significant co-expression relationships. This analysis revealed a dense subnetwork of interconnected hub genes involved in cytoskeletal and ciliary remodeling (*DNAH5*, *FMN2*, *DNAH14*, *FRAS1*)[40-42], signal transduction and scaffolding (*ADCY2*, *MAGI1*)[43,44], transcriptional and post-transcriptional regulation (*SAMMSON, HELLPAR*)[45], and ubiquitin-mediated proteolysis (*HECW1*). [46] Of these, six genes (*ADCY2*, *DNAH14*, *DNAH5*, *HELLPAR*, *MAGI1*, and *FMN2*) were significantly upregulated in the Older* cohort under LPS stimulation. Of these hub genes the most intriguing candidate was ADCY2 which encodes adenylate cyclase 2 which catalyzes the formation of cAMP a secondary messenger important for neuronal signaling[44].

Interestingly, pathway enrichment analysis (Figure 7d) of genes in the Blue module were consistently enriched in pathways related to the neuronal system (e.g., neuroactive ligand-receptor interaction), structural and extracellular matrix dynamics (e.g., ECM organization, collagen biosynthesis and degradation), and immune-related signaling (e.g., interferon gamma response, complement activation).

The pathway enrichment analysis for each module revealed distinct biological processes. The turquoise module, the largest with 1,921 genes, displayed minimal Z-score variation across cohorts and conditions, suggesting that its transcriptional activity was shared by all cohorts. Pathway enrichment analysis highlights consistent activation of pathways associated with immune response regulation, inflammation, and cytokine signaling across KEGG, Reactome, and MSigDB HALLMARK databases. Prominent pathways include cytokine-cytokine receptor interaction**,** chemokine signaling pathway**,** interleukin signaling**,** Toll-like receptor (TLR) signaling**,** and TNF signaling via NF-κB (Supplementary Figure 14).

The brown module (178 genes) showed significant elevation in the Older group versus Young (Supplementary Figure 15b, and Supplementary Figure 13). Pathway enrichment analysis revealed strong associations with platelet biology, coagulation, and vascular homeostasis. Key pathways included: platelet activation, platelet adhesion to exposed collagen, fibrin clot formation, and the response to elevated platelet cytosolic Ca2+ (Supplementary Figure 15b). Finally, the yellow module, consisting of 44 genes, demonstrated significant elevation in both HIV-Young ($p = 0.020$) and Older ($p = 0.031$) cohorts relative to Young controls (Supplementary Figure 16c, and Supplementary Figure 13). Pathway enrichment analysis identified strong associations with innate immunity and antimicrobial defense mechanisms. Prominent pathways included neutrophil degranulation, defensins, antimicrobial peptides, and metal sequestration by antimicrobial proteins (Supplementary Figure 16).

Finally, we performed upstream regulators analysis of all cohorts using Ingenuity Pathway Analysis(Qiagen). Most cohorts seemed to have similar upstream activating and inhibitory regulators, except the Older* cohort which followed a different pattern. An interesting upstream regulator that emerged as inhibited was Suppressor of Cytokine Signaling (SOCS1) which was significantly inhibited in all cohorts except the HIV-Older and Older* cohort. SOCS1 is a known negative regulator of sepsis and the response to LPS[47]. Other interesting upstream regulators included IFNB1 (Supplemental Figure 17), ACOD1, F3, USP18, and SERPINB7; further investigation is needed to determine the role of these proteins in age-associated immune regulation.

Discussion

The NLRP3 inflammasome is an innate immune sensor that plays an important role in fighting infections and is strongly linked to the development of age-related diseases[13-16]. Aged NLRP3 knockout mice show extension of health span when compared to aged wild-type mice [17]. Dysregulation of the NLRP3 inflammasome likely contributes to the proinflammatory environment seen in both aging[17] and HIV-infection[48]. However, it is not completely understood how inflammasome activation is modulated by chronic disease, aging, and HIV-infection. This study set out to understand NLRP3 inflammasome activation at the intersection of HIV-infection and aging through the study of PBMCs and monocytes isolated from four cohorts, HIV-negative young (Young), HIV-positive Young (HIV-Young), HIV-negative Older (Older), HIV-positive Older (HIV-Older), and Older* (a cohort recruited to better match co-morbid conditions in the HIV-Older cohort.

HIV-negative young adults were used as a control and comparison for our older cohorts. We found that HIV-negative young adults (Young) demonstrated low inflammasome activation at baseline, with low caspase-1 activation, and low cytokine levels (IL-1β and IL-18) in all

monocyte subsets (Figure 1), when compared to all other cohorts. With stimulation we saw an appropriate response with an increase in production of IL-1β and IL-18 (Figure 2). With our older cohorts, particularly the HIV-Older cohort and the Older * cohort, we saw evidence of increased inflammasome activation at baseline, characterized by increased caspase-1 activation (Figure 1a-d), and elevated baseline cytokines (IL-1β, IL-18, TNF-α, etc). With stimulation (both LPS and LPS+ATP) we saw an attenuated response with a trend of decreased cytokine production, including IL-1β and IL-18 (Figure 2e). Overall, the HIV-negative young cohort followed a trajectory of inflammasome activation that was also mirrored in the transcriptional data of isolated monocytes with LPS stimulation. All Older adults similarly followed the coordinated trajectory of increased expression of inflammasome genes at the transcriptional level with LPS stimulation, although decreased levels of IL-1B and CASP1 (Figure 5) was noted compared to the Young cohort. In contrast we saw an attenuation of cytokine production with LPS stimulation via flow cytometry (Figure 2). Therefore, HIV-positive older and Older* exhibited a decoupling at the protein level: elevated baseline inflammasome activation but an attenuated response to stimulation. A decoupling of RNA and protein expression has been noted with aging in a number of studies[37,38]. It is possible that post translational modifications are driving the differences we see across our cohorts[39]. Of note, we were only able to sequence purified monocytes after LPS stimulation. It is possible that the LPS+ ATP stimulation could differ at the transcriptional level.

Clinically both older adults and PLH are known to have worse outcomes with infections [49-51]. The attenuation we saw with stimulation in older adults with HIV, and co-morbid conditions could partly explain why these populations may mount ineffective responses to diverse pathogenic threats, including bacterial, viral, and fungal challenges. Age-related reductions in cytokine responsiveness to immune stimulation has been previously noted in older adults—in both dendritic cells[52] and in T cells [53], again showing this pattern of an elevated baseline and a

583 subsequent dampened response. The production of IL-1β is also an important part of mounting
584 a fever—older adults have been shown to have impaired febrile responses in a number of
585 infections[54,55].

586 The increased caspase-1 activation seen at baseline in the older cohorts could reflect
587 increased DAMPs (Damage associated molecular patterns) in the extracellular and cellular
588 milieu seen with aging, along with residual viral patterns despite ART[56-59]. The mechanisms
589 underlying the attenuated response seen in older adults with HIV-infection and co-morbid
590 conditions are likely multifactorial, and could differ by age, HIV-infection and co-morbid
591 conditions. To begin with, the chronic baseline inflammasome activation seen in these subjects
592 could lead to feedback mechanisms that inhibit subsequent activation of the inflammasome in
593 these subjects. One possibility is an IL-10 feedback mechanism. Interestingly, with signal one
594 (LPS) and signal two (LPS+ATP) there was a clear induction of IL-10 noted in certain individuals
595 (Supplementary Figure 5). Elevated levels of IL-10 were observed at baseline in inflammatory
596 and non-classical monocytes from the HIV-negative older cohort with increased co-morbid
597 conditions (Older*), as well as in non-classical monocytes from HIV-positive older adults (HIV-
598 Older)(Supplementary Figure 3). IL-10 has been found to be a regulatory mechanism for
599 prolonged inflammasome activation[11], and has been previously reported as markedly elevated
600 in monocytes from Older individuals compared to the Young[60]. Another possible mechanism
601 could be metabolic pathways induced with LPS stimulation. ACOD1 was the top negative
602 upstream regulator noted across cohorts. ACOD1 encodes cis-aconitate decarboxylase, a
603 mitochondrial enzyme that produces itaconate. Itaconate has been shown to be a key regulator
604 of the NLRP3 inflammasome after prolonged LPS priming.[61] Finally, the attenuated cytokine
605 response noted in older cohorts via flow cytometry could reflect age, HIV- and cohort-
606 associated differences in cell permeability and cell death with stimulation. Young monocytes
607 could be less permeable (less leaky) than monocytes from older adults under LPS and LPS+

ATP stimulation. Additionally, monocytes in older adults could have an increased propensity for cell death. Therefore, there may be age and HIV-associated differences in secretion of IL-1β that maybe influenced by differences in Gasdermin-D regulation, cell permeability and the induction of cell death by cohort. Single cell secretion studies of monocytes from these different cohorts are needed to really answer these questions. We saw a trend of increased cell death as measured by LDH release assay in total PBMCs following LPS stimulation in the Older* and HIV-Older cohort (data not shown) as compared to the younger cohorts but will need to recruit more subjects to fully answer these questions.

We set out to further delineate underlying mechanisms for these differences in inflammasome activation by performing RNA seq of purified monocytes from our different cohorts in the setting of LPS stimulation. Our analysis showed expected shared inflammatory pathways among the cohorts in response to LPS stimulation as shown by our PCA analysis (Figure 4, Figure 7). However, at baseline we saw an upregulation of the Hallmark interferon gamma response and interferon alpha response in the HIV-positive older (HIV-Older) and HIV-negative older cohort with increased co-morbid conditions (Older*) when compared to the HIV-negative young cohort (Figure 6a). With LPS stimulation we saw persistent expression of IFN signaling that was less responsive in the older cohorts with HIV infection and co-morbid conditions compared to the younger cohorts (Figure 6b, Supplementary Figure 11c). Interferon signaling has been noted to be increased in studies of aged mice in almost all mouse tissues [62,63]. This increased basal elevation of interferons has been suggested to be a response to activation of LINE elements, a family of transposable elements[64]. The decline in control of transposons with aging has been posited to contribute to age-related dysfunction and the pro-inflammatory environment associated with aging[62]. Treatment with nucleoside reverse-transcriptase inhibitors (NRTIs) has been shown to decrease transposal element transposition,

dampen the IFN response and extend the lifespan of aging mice and *Drosophila*[65,66]. Interestingly, in our dataset both the HIV-Older group and the Older* cohort, had increased IFN signaling at baseline.

Persistent upregulation of Interferon signaling is a well-known phenomenon in chronic HIV-infection, and there is evidence from prior studies that this interferon persistence may be related to monocyte activation[67]. Here we provide evidence that purified monocytes from older adults with HIV-infection have increased interferon signaling at baseline-- a pattern also noted in HIV-negative older adults with increased co-morbid conditions (Figure 6, Supplementary Figure 11). After stimulation we see persistent IFN signaling (although dampened) in these same cohorts. Our prior work also demonstrated a persistent IFN signature after Dectin-1 stimulation (an innate immune receptor that can recognize both fungal and self-ligands), and increased production of IFN-α in response to Dectin-1 stimulation from dendritic cells and monocytes in the setting of increased age and HIV-infection [68]. IPAnalysis of our data predicted that interferon signaling genes such as IFN-B, ISG15, USP18, and SERPINB7were significant upstream regulators (Supplementary Figure 17b,c). There is evidence that Type I IFN signaling can cause inflammasome suppression[12]. Therefore, the baseline IFN signature in older adults with HIV-infection and co-morbid conditions could also contribute to the dampened inflammasome response seen in these cohorts. Further studies are needed to evaluate this hypothesis.

We conducted pathway enrichment analysis on the unique DEGs in each cohort to identify cohort specific differences with LPS stimulation. Figure 6 (c,d) shows pathways that predominated in specific cohorts. Strikingly, the HIV-Older cohort exhibited selective downregulation of *FADD*, *TICAM2*, *MAPK14*, *BTRC*, and *GSDMD* expression—all genes involved in TLR 4 signaling. The Older* cohort showed upregulation of a neuronal signature,

which included upregulation of specific neuronal receptors such as Opioid receptor mu 1 (OPRM1), GABA receptor 3 (GABRB3), and GRM1 (Glutamate Metabotropic receptor 1), (Supplementary Figure 13). WGCNA analysis helped to further organize divergent pathways among the cohorts into specific modules (Figure 7). The Blue module showed increasing activity along the hypothesized inflammaging trajectory (Young> HIV-Young > HIV-negative Older, HIV-Older, and Older*). This module was enriched in immune pathways such as T cell receptor signaling pathway, PD-1 signaling, and in the Hallmark complement and interferon gamma pathways. Interestingly, it was also enriched for extracellular matrix (ECM) organization pathways as well as pathways related to Neuroactive ligand receptor interaction, Neuronal system, and Nicotine addiction pathways (as seen with our previous analysis of unique DEGs, Figure 6c). Genes that were upregulated were neuroreceptors such as *CNR1* (Cannabinoid receptor 1), *GRM1* (Glutamate receptor 1), *GRM2* (Glutamate receptor 2), *GRM7* (Glutamate receptor 7), *OPRM1* (Opioid receptor mu 1), *GABRB3* (GABA receptor 3), *GABRA2* (GABA subunit 2), *GRIN2B* (a component of NMDA receptor), and *NPFFR1* (Neuropeptide FF receptor 1) (Supplementary Figure 12). These genes were particularly increased in the Older * cohort. Review of the literature shows that there are no reports of GRM1, GRM7, GRIN2B expression in monocytes, thus making this the first notable report. However, there is evidence that fully functional GABA receptor machinery is present in monocytes and is involved in cytokine release, chemotaxis, and in autophagy[69]. Specifically, there is evidence that GABA signaling in macrophages sustains inflammasome activation[70]. There, is also good evidence that both opioid and cannabinoid receptors are expressed in immune cells and can modulate immune function. Specifically, μ-opioid receptor activation has been shown to inhibit NLRP3 inflammasome activity[71], and cannabinoid receptor signaling suppresses immune activation[72,73,74]. The increased expression of neuronal receptors in the high-comorbidity Older* cohort may represent a compensatory mechanism to counterbalance chronic inflammation. This intriguing 'neuro-immune signature' raises the possibility that age-related comorbidities drive the

683 upregulation of endogenous immunomodulatory systems as a feedback response to persistent
684 inflammasome activation. Interestingly, a transgenic mouse model that expresses a caspase-1
685 biosensor examined age-associated inflammasome activation and found aged mice that were
686 treated with LPS showed significant brain inflammation[75]. Additionally, aged female mice have
687 been noted to have higher markers of inflammasome activation in the cortex, compared to aged
688 male mice in models of aging[76]. Therefore, it is also possible that the neural signature we see in
689 older adults is linked to brain inflammation. Further studies are needed to understand the age-
690 related upregulation of these neuronal signatures.

691 Finally, review of all the older cohorts showed that they had distinct immune and
692 transcriptional profiles (Supplementary Figure 7, Figure 6). The Older * cohort often emerged
693 with a unique profile when compared to the other older cohorts. Review of overall co-morbid
694 counts did not show a significant difference between the older cohorts, although all had
695 significantly higher co-morbid conditions than the young cohorts (Supplementary Figure 8, Table
696 3). The older cohorts differed by distribution of biological sex, and race/ethnicity. The Older*
697 cohort had a larger predominance of females (81.8%) compared to the other older cohorts
698 where males dominated (Table 3) which could have contributed to the distinct profiles. There is
699 growing evidence that inflammasome activation differs in females compared to males[77]. For
700 example, in a study using a mouse model of atherosclerosis, loss of NLRP3 inflammasome
701 function attenuated atherosclerosis in female mice but not in male mice—suggesting that
702 inflammasome activation preferentially accentuates atherosclerosis in females[35]. With respect
703 to specific co-morbid conditions, the older cohorts did differ significantly by the distribution of the
704 inflammatory cluster (autoimmune disease, colitis, thyroid disease, osteoarthritis) and organ
705 failure (liver and kidney disease) cluster (Table 3)—the HIV-negative older cohort had 90%
706 predominance of the inflammatory cluster, and 0% of the organ failure cluster (most dominant in
707 the HIV-positive older cohort). When the Older* cohort was further compared to the all the

other older cohorts (Table 4) we saw a significant increase in COPD, as well as a trend of increased current smoking in the Older* cohort. Smoking and COPD are associated with increased inflammasome activation[78,79]. It is possible that these co-morbid conditions, along with biological sex contribute to the higher baseline inflammasome activation and distinct immune/transcriptional profile seen in this cohort. Overall, these studies demonstrate that co-morbid conditions, age, sex, and HIV-infection all contribute to an individual's immune response and deserve further investigation in the future with larger validation cohorts.

Overall, our results highlight distinct inflammatory and transcriptional programs depending on age, HIV-status and co-morbid conditions which deserve further investigation. More studies are needed to unravel these age- and HIV-associated differences as these regulatory mechanisms could differ by cohort or even individual. The differences noted between transcription and protein expression in older adults alludes to the possibility that post translational modifications may be an important driver of these age-associated differences. Post-translational modifications[39], micro-RNAs, and long-coding RNAs[27] need to be further explored in the context of age, HIV-infection and co-morbid conditions. Finally, understanding how age, HIV-infection and co-morbid conditions affects inflammasome activation will be important as inflammasome inhibitors[80] are being used clinically for various conditions. These future studies will be crucial to the future of personalized medicine.

Figure Legends

Figure 1 | Caspase-1 activity and cytokine profiles in monocyte subsets at baseline across cohorts.

(a–d), Caspase-1 activity measured by FAM-FLICA mean fluorescence intensity (MFI) in four monocyte subsets (Activated: $CD11b^{+}CD14^{+}$; Classical:$CD14^{+}CD16^{lo}$; Inflammatory: $CD14^{+}CD16+$; Non-classical:$CD14^{+}CD16^{H}$) from five cohorts: HIV-negative young (Young-blue), HIV-positive young (HIV-Young -green), HIV-negative older (Older -red), HIV-positive older (HIV-Older -purple), and HIV-negative older cohort with increased co-morbidities (Older* -orange). Individual data points and mean ± standard error of the mean (SEM) are shown. Statistical differences were assessed by Kruskal-Wallis test with significance indicated as $*p < 0.05$, $**p < 0.01$, and $***p < 0.0001$. The Young cohort exhibited the lowest caspase-1 activity across all subsets, whereas HIV-Young, HIV-Older, and Older* groups showed significantly elevated levels.

e), Radar plots depicting relative cytokine profiles (z-scores) for monocyte subsets across cohorts. Each axis represents a cytokine, enabling direct comparisons. Dashed grey reference lines at z = –2, 0, and 2 serve as reference points for relative cytokine expression levels. HIV-negative young (Young-blue), HIV-positive young (HIV-Young -green), HIV-negative older (Older -red), HIV-positive older (HIV-Older -purple), and HIV-negative older cohort with increased co-morbidities (Older* -yellow).

Figure 2 | Caspase-1 activation and cytokine profiles in monocyte subsets following LPS (Signal 1) and LPS+ATP (Signal 2) stimulation across cohorts.

(a–d), Caspase-1 activity was assessed by FAM-FLICA staining in four monocyte subsets: activated ($CD11b^{+}CD14^{+}$) (a), classical ($CD14^{+}CD16^{lo}$) (b), inflammatory ($CD14^{+}CD16^{+}$) (c), and non-classical ($CD14^{+}CD16^{H}$) (d) monocytes. Cells were stimulated under two conditions: Signal 1 (LPS alone, represented by solid circles) and Signal 2 (LPS + ATP, represented by open squares), and analyzed across five cohorts: HIV-negative young (Young-blue), HIV-positive young (HIV-Young -green), HIV-negative older (Older -red), HIV-positive older (HIV-Older -purple), and HIV-negative older cohort with increased co-morbidities (Older* -orange).

Grey # indicates statistical significance differences with signal 1 between different cohorts. Black # indicates statistical differences with signal 2 between different cohorts. Finally, Black bars without boundary indicate significant differences within each cohort between signal 1 signal2 (*p<0.05). Data are presented as mean ± SEM. Statistical analyses were performed using the Kruskal-Wallis test with Dunn's post hoc correction for multiple comparisons and the Mann-Whitney U test for selected pairwise comparisons, as appropriate. # p < 0.05, ##p < 0.01, ###p < 0.001, and ####p<0.0001.

e, Radar plots showing standardized cytokine responses (z-scores) under LPS, and LPS+ATP stimulation in five cohorts: Young (blue), HIV-Young (green), Older (red), HIV-Older (purple), and Older* (yellow). Each row corresponds to a distinct monocyte subset, with individual cytokines plotted along the radial axes. Solid lines indicate responses to LPS; dashed lines indicate responses to LPS+ATP. Z-scores were derived from the mean and standard deviation of cytokine-specific percentage changes across all conditions and cohorts. Dashed grey reference lines at z = –2, 0, and 2 serve as reference points for relative cytokine expression levels.

Figure 3. **Age and HIV-infection Interactions**. Age effect (older − younger) (A, B) and HIV effect (HIV Positive − HIV Negative) (C, D) on z transformed response (Δ SD; adjusted for sex and race/ethnicity, averaged over their levels with equal weight). (**A, C)** Main effect for each cell (panel), marker (row) and stimulation (column); red = higher in older (A) or HIV-positive (C), blue = lower. Symbols denote significance of the main effect: * < 0.05, † < 0.01, ‡ < 0.001. (**B, D)** Plots of main effect and interaction on shared axes, Each point represents a feature with a significant effect; point shape gives the marker with adjacent cell label and stimulation . X-axis = main effect (the average of the effect in (B) HIV Negative and HIV Positive) or (D) younger and older); y-axis = interaction (the effect in (B) HIV Positive − effect in HIV Negative or (D)older − younger). The dashed horizontal line represents no interaction and the dotted vertical line represents no main effect. Amplication effects where: the effect is larger in (B) HIV Positive or

in (D) older (amplified) are found in upper right and lower left; Attenuation effects where: the negative effect is larger in the (B) HIV Positive or in (D) older. Crossover effects where the subgroups (B) HIV-positive, HIV-negative and (D) Older, younger have opposite signs (both simple effects $p < 0.05$ are found in top-middle/bottom-middle); Black point = significant main effect only. Green = Attenuated effect, Blue= Amplified Effect Orange/brown= Crossover Effect, The color-coded interaction effects are also specified on the heat maps (A/B) as outlines. Solid line indicates a significant interaction, dashed lines indicate the effect was only significant in a simple effect. Highlighting uses unadjusted p value (no multiple-comparison correction was done).

Figure 4 | Principal component analysis (PCA) and pathway enrichment of bulk RNA-seq data from CD14$^+$ monocytes across five cohorts.

(a), PCA of transcriptional profiles from CD14$^+$ monocytes isolated from five cohorts, stimulated with LPS for 6 hours or left untreated. PC1 (65% variance) captures the dominant effect of LPS stimulation, separating control and LPS-treated samples. PC2 (7% variance) reflects cohort-specific transcriptional differences (color denotes cohort).

(b), Heatmap of enriched MSigDB Hallmark pathways for the top genes driving the first five principal components (PCs), based on gene rankings by PCA loadings. Color intensity indicates $-\log_{10}$(p-value), with red representing positive enrichment and blue representing negative enrichment. PC1 is enriched for inflammatory pathways such as TNFα signaling via NF-κB and interferon responses, reflecting the LPS-induced activation. PC2 is enriched for DNA repair and the unfolded protein response, and PC5 for cholesterol homeostasis—both representing cohort-specific biological variation. PCs 3 and 4 show enrichment for pathways including oxidative phosphorylation, complement activation, mTORC1 signaling, protein secretion, and allograft rejection but are not significantly associated with either stimulation or cohort identity.

(c), PCA restricted to Young and Older cohorts reveals age-dependent transcriptional clustering. PC1 (62.2% variance) separates control and LPS conditions; PC2 (6.9% variance) discriminates age groups under both conditions.

(d), Heatmap of MSigDB Hallmark pathway enrichment for top genes in PCs from the Young and Older cohorts, following the conventions noted in (b). PC1 was strongly associated with LPS stimulation ($p= 1.25 \times 10^{-8}$), while PC2 is significantly associated with age ($p=1.12 \times 10^{-3}$), while the other PCs did not correlate with either age or LPS stimulation.

Figure 5 | Inflammasome-related gene expression in CD14$^+$ monocytes across age groups and stimulation conditions. Panel (a), Heatmap of normalized expression (row Z-score) for 30 selected inflammasome-related genes across samples grouped by cohort (Young, HIV-Young, Older, HIV-Older, Older*) and Condition (Control or LPS). Genes are clustered by expression pattern, highlighting transcriptional changes associated with aging and HIV under basal and LPS-stimulated states. Panel (b-e) CD14$^+$ monocytes were purified and stimulated with LPS for 6 hours. Transcript levels of *IL1B* (b), *CASP1* (c), *CASP4* (d), and *CASP5* (e) were quantified by RT-qPCR. Fold change was calculated relative to matched unstimulated controls using the ΔΔCt method. Fold change after LPS stimulation was assessed within cohorts by one-sample t-tests or Wilcoxon signed-rank tests (*$p < 0.05$, **$p < 0.01$). For *IL1B* (b), expression increased significantly post-LPS in Young, HIV-Young, and Older, and HIV-Older, as indicated by *. Between-cohort comparisons were performed with Mann–Whitney U tests and denoted by #. LPS-induced *IL1B* expression was lower in Older (#$p < 0.05$), HIV-Older (##$p < 0.01$), and Older* (#$p < 0.05$) compared to Young. For *CASP1* (c), although within-cohort upregulation was not significant, Young showed greater fold change than Older (#$p < 0.05$). Both *CASP4* (d) and *CASP5* (e) were significantly upregulated after LPS stimulation in HIV-Young, Older, and HIV-Older cohorts (*$p < 0.05$). In addition, *CASP4* (d) were significantly upregulated after LPS stimulation in Young (*$p < 0.05$). Mann–Whitney tests indicated *CASP5* expression was higher

in Older* compared to Young (#$p < 0.05$). Overall, *CASP4* and *CASP5* exhibited similar cohort-specific expression patterns.

Figure 6 | Transcriptomic pathway enrichment and gene overlap analyses across cohorts.

a), Dot plot displaying significantly enriched Hallmark pathways from DESeq2 comparisons of unstimulated groups (baseline). The y-axis shows enriched pathways; dot size represents significance ($-\log_{10}$ adjusted p-value, adj. $p < 0.05$); dot color indicates Normalized Enrichment Score (NES), with red denoting upregulation in the first-named group and blue indicating downregulation.

b), Dot plot showing cohort-modulated LPS responses from DESeq2 interaction analysis testing whether LPS effects differ by age/HIV status. The x-axis shows the comparison of the delta (change from baseline with LPS stimulation) in each cohort vs. delta in young or the older cohort (after dotted line) (e.g., Δ HIV-Young vs Δ Young). Dot size and color follow panel (a), with red indicating stronger LPS induction relative to Young, and blue indicating attenuation. Dashed vertical lines separate comparison categories.

c), Bubble plot showing pathway enrichment results of upregulated, cohort-specific differentially expressed DEGs in the Older*, HIV-Young, and Young cohorts. Pathways are listed on the y-axis; cohorts are shown on the x-axis. Bubble size represents fold enrichment and bubble color indicated statistical significance (-log10(FDR)) respectively. Pathways with fewer than four associated genes were excluded.

d), Bubble plot showing pathway enrichment results of downregulated, cohort-specific differentially expressed DEGs in the Older* and HIV-Older cohorts. Pathways are listed on the y-axis; cohorts are shown on the x-axis. Bubble size represents fold enrichment and bubble

color indicated statistical significance (-log10(FDR)) respectively. Pathways with fewer than four associated genes were excluded.

Figure 7 | Co-expression modules identified by WGCNA and their age- and condition-specific expression profiles.

a), Gene dendrogram and module color assignments derived from weighted gene co-expression network analysis (WGCNA). Genes were hierarchically clustered based on expression similarity using a soft threshold power of 5 and a minimum module size of 20. Four co-expression modules were identified: Brown (178 genes), Yellow (44 genes), Blue (853 genes), and Turquoise (1921 genes). The upper panel shows the dendrogram, where the x-axis denotes individual genes and the y-axis represents the clustering height (dissimilarity). The lower panel color-codes the resulting modules using dynamic tree cut, with each branch representing a unique gene co-expression cluster.

b), Expression trajectories of genes within each module across age groups and stimulation conditions (Control vs. LPS). For each module (Brown, Yellow, Blue, Turquoise), gene expression is Z-score normalized. The x-axis indicates the five age-defined cohorts (Young, HIV-Young, Older, HIV-Older, and Older*), while the y-axis shows Z-scored expression. Thin lines represent individual gene trajectories under Control (blue) and LPS (red) conditions; bold lines indicate the average trajectory for each condition. These plots reveal condition-specific and cohort-dependent expression dynamics.

c), Gene interaction network of top enriched genes within the Blue module. Nodes represent individual genes, and edges denote known physical or functional interactions. Key hub genes, including HELLPAR, FRAS1, and DNAH14, are centrally positioned, suggesting pivotal roles in the regulation of pathways enriched in this module.

d), Pathway enrichment analysis for the Blue module. A bubble plot visualizes significantly enriched pathways derived from KEGG (beige), Reactome (orange), and Hallmark (grey-blue)

databases. Bubble size reflects the number of genes involved in each pathway, while color intensity indicates enrichment significance ($-\log_{10}$[FDR]), with red denoting higher significance. Notable pathways include "Neuronal System," "ECM-Receptor Interaction," "Hematopoietic Cell Lineage," and "Collagen Degradation."

Methods

Clinical study design

We recruited a total of 150 HIV-negative and HIV-positive participants, divided between young (21-35) and older (≥ 60 years) adults. Subjects were recruited from the Yale Health Plan, Yale Primary Care Center (PCC), and the Nathan Smith HIV Clinic (now Yale Center for Infectious Diseases). Participants were evaluated for clinical characteristics by chart review and self-report for demographic information, medications, CD4 count, HIV viral load, and comorbid conditions. 147 subjects were used for all studies combined, including the initial flow cytometry studies, the western blot studies, and the follow up studies. These clinical attributes are summarized in Table 1, Table 2, Table 3, and Table 4. Traditionally, the Yale Health Plan subjects represented a healthier group of subjects, compared to the Yale Primary Care Center (PCC) and the HIV clinic. This study was approved according to a protocol approved by the Human Research Protection Program of the Yale School of Medicine. Informed consent was obtained from all subjects prior to participation.

Sample preparation and Flow Cytometry Analysis

Peripheral blood mononuclear cells (PBMCs) were isolated from heparinized blood using BD Vacutainer® CPT™ Mononuclear Cell Preparation Tubes (BD Biosciences), following the manufacturer's instructions[81]. Freshly isolated PBMCs (5×10^5) were seeded in 96-well plates

containing RPMI 1640 medium. For stimulation, PBMCs were treated with 1 µg/mL of the TLR4 agonist lipopolysaccharide (LPS) for 6 hours. For signal 2 stimulation, 5 mM of ATP was added after 3 hours of LPS incubation and further incubated for 20 minutes. After the 20 mins the plates were washed, spun and replaced with new media—and allowed to incubate for another 3 hours. After stimulation, cells were stained with surface antibodies to identify and classify monocyte subsets. The following antibodies were used: anti-CD14 PE-CF594 (clone M5E2, BD Biosciences), anti-CD16 BV510 (clone 3G8, BD Biosciences), and anti-CD11b APC-Cy7 (clone ICRF44, BD Biosciences). Cells were then fixed using Cytofix™ buffer (BD Biosciences) and stored at −80 °C in freezing medium until analysis. On the day of flow cytometry, cells were thawed, washed, and permeabilized using Cytofix/Cytoperm™ and Perm/Wash buffer (BD Biosciences). Intracellular cytokine staining was performed using the following antibodies: anti-IL-18 Pacific Blue (clone D2F3B, Cell Signaling Technology), anti-TNF-α BV750 (clone MAb11, BD Biosciences), anti-IL-6 PE-Cy7 (clone MQ2-13A5, eBioscience), anti-IFN-β FITC (clone MMHB-3, PBL), and anti-cleaved IL-1β Alexa 700 (clone D3A3Z, Cell Signaling Technology—this antibody was custom made for our studies). Samples were run using a cytoFLEX flow cytometer (Beckman coulter) and analyzed using FlowJo software (FlowJo, LLC).

Caspase-1 FLICA experiment

PBMCs were pre-treated with FAM-FLICA (FAM-YVAD-FMK) which contains a caspase-1 inhibitor (YVAD) sandwiched between a green, fluorescent label (carboxyfluorescein, FAM), providing a rapid and flexible method for analyzing active caspases (ImmunoChemistry Technology, MN). LPS primed PBMC (3 hours) were incubated with activated Caspase 1 binding peptide z-VAD-FMK (FLICA) (ImmunoChemistry Technology, MN) along with ATP (5mM) for 20 minutes and washed with culture media to remove excess ATP in culture. Washed PBMC were further incubated at 37^0C for additional 3 hours supplemented with culture media. Following activation and labelling of activated Caspase 1 using FLICA, PBMC samples were

washed with 1x FACS buffer (PBS containing 2% FBS) stained for monocyte surface markers as noted above.

Monocyte isolation and RNA-seq

Untouched human primary monocytes were purified by negative selection using a Dynabeads kit (Invitrogen), yielding an average 98% purity. Freshly isolated monocytes were cultured in RPMI 1640 supplemented with 10% heat-inactivated FBS and antibiotics and used in experiments after being stabilized for at least 1 hour and subsequently stimulated for 6 hours with LPS. Total RNA was extracted from isolated human primary monocytes according to manufacturer's protocol for the RNeasy kits, respectively (Qiagen). The library preparation and sequencing were performed in Yale Stem Center Genomics Core Facility by Dr. Mei Zhong. The raw FASTQ files were executed for adaptor trimming and quality trimming using Cutadapt v1.18[82]. The quality control of the raw and trimmed FASTQ files were performed using FASTQC v0.11.7[83] The trimmed files were aligned to human genome reference (GRCh38.primary assembly) by using STAR/ 2.7.3a-foss-2018b with parameters –runThreadN 12 --outFilterMultimapNmax 1 --outFilterMismatchNmax 999 --outFilterMismatchNoverLmax 0.02 --alignIntronMin 20 --alignIntronMax 1000000 --alignMatesGapMax 1000000 --sjdbOverhang 100 --outSAMtype BAM SortedByCoordinate[84]. The BAM files were further sorted using SAMtools/1.9-foss-2018b and raw counts were obtained using Subread/2.0.0-GCC-7.3.0-2.30 featureCounts package and gencode v29 annotation.

RT-qPCR

Peripheral blood mononuclear cells (PBMCs) isolated from five cohorts and total RNA was extracted using TRIzol reagent (Invitrogen) and reverse-transcribed into cDNA using a high-

capacity cDNA synthesis kit. Gene expression levels of *CASP1*, *CASP4*, *CASP5*, and *IL1B* were measured using SYBR Green qPCR and normalized to GAPDH using the ΔΔCt method.

Bioinformatic Analyses

Transcriptomic profiling data were analyzed using Gene Set Enrichment Analysis (GSEA) to identify significantly enriched pathways related to inflammasome activation and cytokine signaling. Weighted Gene Co-expression Network Analysis (WGCNA) was used to identify co-expression modules correlated with clinical variables such as age, HIV status, and cytokine expression levels. KEGG and GO pathway databases were used for functional annotation. Analyses were performed in R using the fgsea, WGCNA, and clusterProfiler packages.

Upstream regulator analysis was integrated as part of the bioinformatics pipeline to uncover transcriptional regulators potentially driving the observed gene expression changes. Differentially expressed genes (DEGs) from five cohorts (Young, HIV-Young, Older, HIV-Older, and Older*) were analyzed using Ingenuity Pathway Analysis (IPA, Qiagen, version 01-23-01). IPA's Upstream Regulator Analysis identified candidate regulators along with activation Z-scores, expression log ratios, p-values of overlap, and predicted activation states.

Regulators were filtered with stringent criteria: p-value < 0.01, |Z-score| ≥ 2, and expression log ratio thresholds of ±3 to focus on strongly regulated factors. Filtered regulators across cohorts were merged by regulator name for comparative analysis. Activation and inhibition signals were separated by clipping positive and negative Z-scores, respectively, and regulators lacking activation or inhibition signals were excluded from respective datasets. Data alignment ensured consistent ordering of regulators for visualization.

Statistical Analyses and Data Visualization

Group comparisons were performed using one-way or two-way ANOVA followed by post-hoc Tukey's or Sidak's test as appropriate. For non-parametric data, the Kruskal-Wallis test was used with post-hoc Dunn's test. Paired comparisons were conducted using Student's t-test or the Wilcoxon matched-pairs test, depending on data normality. Correlations between gene expression and clinical metadata were assessed by Pearson or Spearman correlation. All p-values were adjusted using the Benjamini-Hochberg method where applicable. Data visualization was performed in Python (Seaborn, Matplotlib) and R (ggplot2), with significance thresholds set at $p < 0.05$.

Statistical Methods for Univariate Model

Data Preparation and Normalization

Inflammatory marker responses were standardized using within-group z-scores computed separately by cell type, marker, and stimulation condition. Unstimulated responses (stim == "base") were z-scored on the logit scale, while stimulated responses were z-scored on the raw scale (represented as the difference in % positive), reflecting their different distributional forms. Observations with an absolute z-score exceeding 3.5 were excluded as outliers prior to modeling. Cell × stimulation × marker combinations with near-zero variance in the response variable were identified and excluded from analysis. Sex and a binary race/ethnicity indicator (White and non-Hispanic vs. non-White or Hispanic) were included as covariates in all models. Chronic medical conditions were summarized in two ways: (1) a continuous comorbidity burden index representing the total count of conditions, and (2) a set of binary cluster indicators denoting the presence of at least one condition within each of six clinically defined groups: **behavioral** (smoking, alcohol abuse, recreational drug use), **metabolic** (obesity (BMI ≥ 30,

diabetes, high cholesterol), **cardiovascular** (hypertension, coronary artery disease (CAD), myocardial infarction (MI), congestive heart failure (CHF), peripheral vascular disease (PVD), arrythmias, valvular disease), **pulmonary** (asthma, COPD, lung disease, sleep apnea), **inflammatory** (autoimmune, colitis, thyroid disease, osteoarthritis) and **organ disease** (kidney disease, liver disease).

Descriptive Statistics

Baseline characteristics were summarized as means (SD) for continuous variables and counts (percentages) for categorical variables. Between-group differences in continuous variables were assessed using one-way ANOVA (with equal-variance assumption); categorical variables were compared using Fisher's exact test.

Age × HIV Factorial Analysis: For every cell × stimulation × marker combination, a linear regression model was fit to the normalized response: (response_z ~ AGE × HIV + sex + race/ethnicity). The Older* cohort was excluded from this stage. Estimated marginal means were obtained and contrasts computed for: (1) the main effect of age (Young vs. Old), (2) the main effect of HIV status (negative vs. positive), and (3) simple effects of the Age × HIV interaction (HIV within each age stratum; Age within each HIV stratum). Within each contrast family, p-values were adjusted using Tukey's HSD (Honestly significant difference). Across all cell × stim × marker combinations, an additional Benjamini–Hochberg (BH) false discovery rate correction was applied within each contrast type.

Cohort Analysis (Older* Comparison): Cell × stimulation × marker combinations that were identified as having a significant HIV effect in the prior analysis were carried forward. The dataset was restricted to older participants only [(HIV-negative Older (Older), HIV-positive Older (HIV-Older), (Older*)], and a linear model was fit: (response_z ~ COHORT + sex + race/ethnicity). All pairwise contrasts among the three cohorts were computed with Tukey's

HSD adjustment; BH correction was applied across combinations. Combinations were flagged if any pairwise contrast involving the Older* cohort reached $p < 0.05$.

Older* Univariate Analysis: In a parallel and independent analysis, the cohort model above was applied to the full set of cell × stimulation × marker combinations, to allow detection of Older*-specific differences not captured by the HIV contrast. To select chronic conditions for the subsequent attenuation analysis, Fisher's exact tests were conducted comparing the prevalence of each individual condition between the Older* and non-Older* groups; conditions with $p < 0.20$ were retained (COPD, osteoarthritis, smoking, arrhythmias, depression, kidney disease, asthma, lung disease).

Attenuation Analysis: For combinations showing a significant cohort difference (Cohort analysis or the Older* analysis), a series of models were fit by sequentially adding one chronic-condition covariate at a time to the base model (COHORT + sex + race/ethnicity). In the factorial pipeline, the comorbidity burden count and each of the six cluster indicators were tested in turn. In the Older* pipeline, the eight individually selected conditions were tested. For each model, the adjusted pairwise mean difference between cohorts was extracted and compared to the unadjusted (base model) estimate. Attenuation was quantified as the proportional reduction in the cohort contrast estimate: Attenuation = (base estimate − adjusted estimate) / base estimate. Substantive attenuation following the inclusion of a given condition was interpreted as evidence of possible confounding or mediation of the inflammatory response by that condition.

Limitations: Our studies were limited by how many human subjects could be recruited. Our follow up studies were limited by funding issues.

Implications and Future Directions: Understanding how age, HIV-infection and co-morbid conditions affects inflammasome activation will be important as Inflammasome inhibitors are being developed and will be used in different human cohorts.

Declarations

This study was approved according to a protocol approved by the Human Research Protection Program of the Yale School of Medicine. Informed consent was obtained from all subjects prior to participation.

The RNA seq data generated by this study will be uploaded to the GEO database once this manuscript is published.

Funding: This work was funded by the NIH/NIA K76AG064548, 3K76AG064548-04S1, the Claude D. Pepper Older Americans Independence Center at Yale (PESC), 2P30AG021342-21, and the Emerging Pathogens Initiative (HHMI).

Author Contributions

S.D. and A.K. contributed equally to this work. S.D. and A.K. performed sample preparation, flow cytometry, and initial RNA seq analyses. S.D. conducted RT-PCR, and final analysis of RNA seq data. B.L. assisted with preliminary processing of sequencing data. A.E. assisted with sample preparation. I.M. recruited blood donors and performed blood collection. B.V.W. analyzed clinical data from donors and performed all statistical analyses. S.D. and H.J.Z. wrote the manuscript. S.D., A.K. and H.J.Z. designed the study. H.J.Z. supervised the study and A.C.S., SD, and H.J.Z. revised the manuscript. CR assisted with organization and entering of clinical variables into our redcap database. LB assisted with recruitment of subjects. ST assisted with data extraction of clinical variables for subsequent statistical analysis. AN assisted with subject recruitment.

Acknowledgements: We would like to acknowledge the patients of the Yale Nathan Smith Clinic (now Yale Center for Infectious Diseases), the Yale Health plan, and the Yale primary

center for their willingness to participate in this study. We would like to also acknowledge Mei Zhong and the Yale Center for Genome Analysis. Finally, we would like to thank Albert Shaw, for his time and feedback in revising this manuscript.

References

1 Smit, M. *et al.* Future challenges for clinical care of an ageing population infected with HIV: a modelling study. *Lancet Infect Dis* **15**, 810-818 (2015). https://doi.org:10.1016/S1473-3099(15)00056-0

2 Guaraldi, G. *et al.* Premature age-related comorbidities among HIV-infected persons compared with the general population. *Clin Infect Dis* **53**, 1120-1126 (2011). https://doi.org:10.1093/cid/cir627

3 Pathai, S., Bajillan, H., Landay, A. L. & High, K. P. Is HIV a model of accelerated or accentuated aging? *J Gerontol A Biol Sci Med Sci* **69**, 833-842 (2014). https://doi.org:10.1093/gerona/glt168

4 Hsue, P. Y. & Waters, D. D. HIV infection and coronary heart disease: mechanisms and management. *Nat Rev Cardiol* **16**, 745-759 (2019). https://doi.org:10.1038/s41569-019-0219-9

5 Jha, S., Brickey, W. J. & Ting, J. P. Inflammasomes in Myeloid Cells: Warriors Within. *Microbiol Spectr* **5** (2017). https://doi.org:10.1128/microbiolspec.MCHD-0049-2016

6 Sharma, B. R. & Kanneganti, T. D. NLRP3 inflammasome in cancer and metabolic diseases. *Nat Immunol* **22**, 550-559 (2021). https://doi.org:10.1038/s41590-021-00886-5

7 Gaidt, M. M. *et al.* Human Monocytes Engage an Alternative Inflammasome Pathway. *Immunity* **44**, 833-846 (2016). https://doi.org:10.1016/j.immuni.2016.01.012

8 Gaidt, M. M. & Hornung, V. Alternative inflammasome activation enables IL-1beta release from living cells. *Curr Opin Immunol* **44**, 7-13 (2017). https://doi.org:10.1016/j.coi.2016.10.007

9 Barnett, K. C. *et al.* An epithelial-immune circuit amplifies inflammasome and IL-6 responses to SARS-CoV-2. *Cell Host Microbe* **31**, 243-259 e246 (2023). https://doi.org:10.1016/j.chom.2022.12.005

10 Alvarez, S. & Munoz-Fernandez, M. A. TNF-Alpha may mediate inflammasome activation in the absence of bacterial infection in more than one way. *PLoS One* **8**, e71477 (2013). https://doi.org:10.1371/journal.pone.0071477

11 Gurung, P. *et al.* Chronic TLR Stimulation Controls NLRP3 Inflammasome Activation through IL-10 Mediated Regulation of NLRP3 Expression and Caspase-8 Activation. *Sci Rep* **5**, 14488 (2015). https://doi.org:10.1038/srep14488

12 Guarda, G. *et al.* Type I interferon inhibits interleukin-1 production and inflammasome activation. *Immunity* **34**, 213-223 (2011). https://doi.org:10.1016/j.immuni.2011.02.006

13 Wen, H. *et al.* Fatty acid-induced NLRP3-ASC inflammasome activation interferes with insulin signaling. *Nat Immunol* **12**, 408-415 (2011). https://doi.org:10.1038/ni.2022

14 Vandanmagsar, B. *et al.* The NLRP3 inflammasome instigates obesity-induced inflammation and insulin resistance. *Nat Med* **17**, 179-188 (2011). https://doi.org:10.1038/nm.2279

15 Robblee, M. M. *et al.* Saturated Fatty Acids Engage an IRE1alpha-Dependent Pathway to Activate the NLRP3 Inflammasome in Myeloid Cells. *Cell Rep* **14**, 2611-2623 (2016). https://doi.org:10.1016/j.celrep.2016.02.053

16 Guo, H., Callaway, J. B. & Ting, J. P. Inflammasomes: mechanism of action, role in disease, and therapeutics. *Nat Med* **21**, 677-687 (2015). https://doi.org:10.1038/nm.3893

17 Youm, Y. H. *et al.* Canonical Nlrp3 inflammasome links systemic low-grade inflammation to functional decline in aging. *Cell Metab* **18**, 519-532 (2013). https://doi.org:10.1016/j.cmet.2013.09.010

18 Franceschi, C. *et al.* Inflammaging and anti-inflammaging: A systemic perspective on aging and longevity emerged from studies in humans. *Mechanisms of Ageing and Development* **128**, 92-105 (2007). https://doi.org:10.1016/j.mad.2006.11.016

19 Franceschi, C., Garagnani, P., Parini, P., Giuliani, C. & Santoro, A. Inflammaging: a new immune-metabolic viewpoint for age-related diseases. *Nat Rev Endocrinol* **14**, 576-590 (2018). https://doi.org:10.1038/s41574-018-0059-4

20 Zicari, S. *et al.* Immune Activation, Inflammation, and Non-AIDS Co-Morbidities in HIV-Infected Patients under Long-Term ART. *Viruses* **11** (2019). https://doi.org:10.3390/v11030200

21 Schnittman, S. R. *et al.* Coronary Artery Plaque Composition and Severity Relate to the Inflammasome in People With Treated Human Immunodeficiency Virus. *Open Forum Infect Dis* **10**, ofad106 (2023). https://doi.org:10.1093/ofid/ofad106

22 Hoel, H. *et al.* Soluble Markers of Interleukin 1 Activation as Predictors of First-Time Myocardial Infarction in HIV-Infected Individuals. *J Infect Dis* **221**, 506-509 (2020). https://doi.org:10.1093/infdis/jiz253

23 Kearns, A. C. *et al.* Caspase-1 Activation Is Related With HIV-Associated Atherosclerosis in an HIV Transgenic Mouse Model and HIV Patient Cohort. *Arterioscler Thromb Vasc Biol* **39**, 1762-1775 (2019). https://doi.org:10.1161/ATVBAHA.119.312603

24 Guo, H., Gao, J., Taxman, D. J., Ting, J. P. & Su, L. HIV-1 infection induces interleukin-1beta production via TLR8 protein-dependent and NLRP3 inflammasome mechanisms in human monocytes. *J Biol Chem* **289**, 21716-21726 (2014). https://doi.org:10.1074/jbc.M114.566620

25 Walsh, J. G. *et al.* Rapid inflammasome activation in microglia contributes to brain disease in HIV/AIDS. *Retrovirology* **11**, 35 (2014). https://doi.org:10.1186/1742-4690-11-35

26 Cao, Y. *et al.* Phenotypic and functional alterations of monocyte subsets with aging. *Immun Ageing* **19**, 63 (2022). https://doi.org:10.1186/s12979-022-00321-9

27 Luo, D. *et al.* Functional crosstalk between Long non-coding RNAs and the NLRP3 inflammasome in the regulation of diseases. *Mol Immunol* **131**, 191-200 (2021). https://doi.org:10.1016/j.molimm.2020.12.038

28 Doitsh, G. *et al.* Cell death by pyroptosis drives CD4 T-cell depletion in HIV-1 infection. *Nature* **505**, 509-514 (2014). https://doi.org:10.1038/nature12940

29 Ziegler-Heitbrock, L. & Hofer, T. P. Toward a refined definition of monocyte subsets. *Front Immunol* **4**, 23 (2013). https://doi.org:10.3389/fimmu.2013.00023

30 Grabarek, J., Amstad, P. & Darzynkiewicz, Z. Use of fluorescently labeled caspase inhibitors as affinity labels to detect activated caspases. *Human Cell* **15**, 1-12 (2002). https://doi.org:10.1111/j.1749-0774.2002.tb00094.x

31 Wang, H. *et al.* IL-6 promotes collagen-induced arthritis by activating the NLRP3 inflammasome through the cathepsin B/S100A9-mediated pathway. *Int Immunopharmacol* **88**, 106985 (2020). https://doi.org:10.1016/j.intimp.2020.106985

32 Franchi, L., Eigenbrod, T. & Núñez, G. Cutting Edge: TNF-α Mediates Sensitization to ATP and Silica via the NLRP3 Inflammasome in the Absence of Microbial Stimulation.

The Journal of Immunology **183**, 792-796 (2009). https://doi.org:10.4049/jimmunol.0900173

33 Diaz-Pino, R. *et al.* Type I interferon regulates interleukin-1beta and IL-18 production and secretion in human macrophages. *Life Sci Alliance* **7** (2024). https://doi.org:10.26508/lsa.202302399

34 Inoue, M. *et al.* Interferon-beta therapy against EAE is effective only when development of the disease depends on the NLRP3 inflammasome. *Sci Signal* **5**, ra38 (2012). https://doi.org:10.1126/scisignal.2002767

35 Chen, S. *et al.* Sex-Specific Effects of the Nlrp3 Inflammasome on Atherogenesis in LDL Receptor-Deficient Mice. *JACC Basic Transl Sci* **5**, 582-598 (2020). https://doi.org:10.1016/j.jacbts.2020.03.016

36 Ge, S. X., Son, E. W. & Yao, R. iDEP: an integrated web application for differential expression and pathway analysis of RNA-Seq data. *BMC Bioinformatics* **19**, 534 (2018). https://doi.org:10.1186/s12859-018-2486-6

37 Solyga, M., Majumdar, A. & Besse, F. Regulating translation in aging: from global to gene-specific mechanisms. *EMBO Rep* **25**, 5265-5276 (2024). https://doi.org:10.1038/s44319-024-00315-2

38 Wei, Y. N. *et al.* Transcript and protein expression decoupling reveals RNA binding proteins and miRNAs as potential modulators of human aging. *Genome Biol* **16**, 41 (2015). https://doi.org:10.1186/s13059-015-0608-2

39 Dufies, O. & Zanoni, I. Post-translational modifications of NLRP3: to prime or not to prime? *Trends Immunol* **47**, 119-129 (2026). https://doi.org:10.1016/j.it.2025.10.008

40 Olbrich, H. *et al.* Mutations in DNAH5 cause primary ciliary dyskinesia and randomization of left-right asymmetry. *Nature Genetics* **30**, 143-144 (2002). https://doi.org:10.1038/NG817;KWRD=BIOMEDICINE

41 Kundu, T., Dutta, P., Nagar, D., Maiti, S. & Ghose, A. Coupling of dynamic microtubules to F-actin by Fmn2 regulates chemotaxis of neuronal growth cones. *Journal of Cell Science* **134** (2021). https://doi.org:10.1242/JCS.252916

42 Vrontou, S. *et al.* Fras1 deficiency results in cryptophthalmos, renal agenesis and blebbed phenotype in mice. *Nature Genetics* **34**, 209-214 (2003). https://doi.org:10.1038/NG1168;KWRD=BIOMEDICINE

43 Hirabayashi, S. *et al.* MAGI-1 is a component of the glomerular slit diaphragm that is tightly associated with nephrin. *Laboratory Investigation 2005 85:12* **85**, 1528-1543 (2005). https://doi.org:10.1038/labinvest.3700347

44 Gray, M., Nash, K. R. & Yao, Y. Adenylyl cyclase 2 expression and function in neurological diseases. *CNS Neurosci Ther* **30**, e14880 (2024). https://doi.org:10.1111/cns.14880

45 Leucci, E. *et al.* Melanoma addiction to the long non-coding RNA SAMMSON. *Nature 2016 531:7595* **531**, 518-522 (2016). https://doi.org:10.1038/nature17161

46 Lin, Y. *et al.* HECW1 induces NCOA4-regulated ferroptosis in glioma through the ubiquitination and degradation of ZNF350. *Cell Death & Disease 2023 14:12* **14**, 1-13 (2023). https://doi.org:10.1038/s41419-023-06322-w

47 Pineros Alvarez, A. R. *et al.* SOCS1 is a negative regulator of metabolic reprogramming during sepsis. *JCI Insight* **2** (2017). https://doi.org:10.1172/jci.insight.92530

48 Bandera, A. *et al.* The NLRP3 Inflammasome Is Upregulated in HIV-Infected Antiretroviral Therapy-Treated Individuals with Defective Immune Recovery. *Front Immunol* **9**, 214 (2018). https://doi.org:10.3389/fimmu.2018.00214

49 van Duin, D. Diagnostic challenges and opportunities in older adults with infectious diseases. *Clin Infect Dis* **54**, 973-978 (2012). https://doi.org:10.1093/cid/cir927

50 Margalit, I. *et al.* Presentation, management, and outcomes of older compared to younger adults with hospital-acquired bloodstream infections in the intensive care unit: a multicenter cohort study. *Infection* **52**, 2435-2443 (2024). https://doi.org:10.1007/s15010-024-02304-y

51 Taramasso, L. *et al.* Bloodstream infections in patients living with HIV in the modern cART era. *Sci Rep* **9**, 5418 (2019). https://doi.org:10.1038/s41598-019-41829-3

52 Panda, A. *et al.* Age-associated decrease in TLR function in primary human dendritic cells predicts influenza vaccine response. *J Immunol* **184**, 2518-2527 (2010). https://doi.org:10.4049/jimmunol.0901022

53 Shen-Orr, S. S. *et al.* Defective Signaling in the JAK-STAT Pathway Tracks with Chronic Inflammation and Cardiovascular Risk in Aging Humans. *Cell Syst* **3**, 374-384 e374 (2016). https://doi.org:10.1016/j.cels.2016.09.009

54 Berman, P. & Fox, R. A. Fever in the elderly. *Age Ageing* **14**, 327-332 (1985). https://doi.org:10.1093/ageing/14.6.327

55 Zheng, H. *et al.* Resistance to fever induction and impaired acute-phase response in interleukin-1 beta-deficient mice. *Immunity* **3**, 9-19 (1995). https://doi.org:10.1016/1074-7613(95)90154-x

56 Cai, C. W. & Sereti, I. Residual immune dysfunction under antiretroviral therapy. *Semin Immunol* **51**, 101471 (2021). https://doi.org:10.1016/j.smim.2021.101471

57 Brenchley, J. M. *et al.* Microbial translocation is a cause of systemic immune activation in chronic HIV infection. *Nat Med* **12**, 1365-1371 (2006). https://doi.org:10.1038/nm1511

58 Franceschi, C., Garagnani, P., Vitale, G., Capri, M. & Salvioli, S. Inflammaging and 'Garb-aging'. *Trends Endocrinol Metab* **28**, 199-212 (2017). https://doi.org:10.1016/j.tem.2016.09.005

59 Shaw, A. C., Goldstein, D. R. & Montgomery, R. R. Age-dependent dysregulation of innate immunity. *Nat Rev Immunol* **13**, 875-887 (2013). https://doi.org:10.1038/nri3547

60 Mohanty, S. *et al.* Prolonged proinflammatory cytokine production in monocytes modulated by interleukin 10 after influenza vaccination in older adults. *J Infect Dis* **211**, 1174-1184 (2015). https://doi.org:10.1093/infdis/jiu573

61 Bambouskova, M. *et al.* Itaconate confers tolerance to late NLRP3 inflammasome activation. *Cell Reports* **34** (2021). https://doi.org:10.1016/j.celrep.2021.108756

62 Cao, W. IFN-Aging: Coupling Aging With Interferon Response. *Front Aging* **3**, 870489 (2022). https://doi.org:10.3389/fragi.2022.870489

63 Benayoun, B. A. *et al.* Remodeling of epigenome and transcriptome landscapes with aging in mice reveals widespread induction of inflammatory responses. *Genome Res* **29**, 697-709 (2019). https://doi.org:10.1101/gr.240093.118

64 Yu, Q. *et al.* Type I interferon controls propagation of long interspersed element-1. *J Biol Chem* **290**, 10191-10199 (2015). https://doi.org:10.1074/jbc.M114.612374

65 Wood, J. G. *et al.* Chromatin-modifying genetic interventions suppress age-associated transposable element activation and extend life span in Drosophila. *Proc Natl Acad Sci U S A* **113**, 11277-11282 (2016). https://doi.org:10.1073/pnas.1604621113

66 Simon, M. *et al.* LINE1 Derepression in Aged Wild-Type and SIRT6-Deficient Mice Drives Inflammation. *Cell Metab* **29**, 871-885 e875 (2019). https://doi.org:10.1016/j.cmet.2019.02.014

67 van Pul, L. *et al.* Human Immunodeficiency Virus-Induced Interferon-Stimulated Gene Expression Is Associated With Monocyte Activation and Predicts Viral Load. *Open Forum Infect Dis* **11**, ofae434 (2024). https://doi.org:10.1093/ofid/ofae434

68 Kumar, A. *et al.* Dectin-1 stimulation promotes a distinct inflammatory signature in the setting of HIV-infection and aging. *Aging (Albany NY)* **15**, 7866-7908 (2023). https://doi.org:10.18632/aging.204927

69 Bhandage, A. K. & Barragan, A. GABAergic signaling by cells of the immune system: more the rule than the exception. *Cell Mol Life Sci* **78**, 5667-5679 (2021). https://doi.org:10.1007/s00018-021-03881-z

70 Xia, Y. *et al.* GABA transporter sustains IL-1β production in macrophages. *Sci Adv* **7** (2021). https://doi.org:10.1126/sciadv.abe9274

71 Cui, X. *et al.* Herkinorin negatively regulates NLRP3 inflammasome to alleviate neuronal ischemic injury through activating Mu opioid receptor and inhibiting the NF-κB pathway. *J Cell Biochem* (2021). https://doi.org:10.1002/jcb.29929

72 Croxford, J. L. & Yamamura, T. Cannabinoids and the immune system: Potential for the treatment of inflammatory diseases? *Journal of Neuroimmunology* **166**, 3-18 (2005). https://doi.org:10.1016/j.jneuroim.2005.04.023

73 Berdyshev, E. V. Cannabinoid receptors and the regulation of immune response. *Chemistry and Physics of Lipids* **108**, 169-190 (2000). https://doi.org:https://doi.org/10.1016/S0009-3084(00)00195-X

74 Grabon, W. *et al.* CB2 expression in mouse brain: from mapping to regulation in microglia under inflammatory conditions. *J Neuroinflammation* **21**, 206 (2024). https://doi.org:10.1186/s12974-024-03202-8

75 Talley, S. *et al.* Characterization of age-associated inflammasome activation reveals tissue specific differences in transcriptional and post-translational inflammatory responses. *Immunity and Ageing* **21** (2024). https://doi.org:10.1186/s12979-024-00462-z

76 Cyr, B. & de Rivero Vaccari, J. P. Sex Differences in the Inflammatory Profile in the Brain of Young and Aged Mice. *Cells* **12** (2023). https://doi.org:10.3390/cells12101372

77 Ciani, M. *et al.* Neuroimmune modulatory effects of the NLRP3 inflammasome: the role of sex and living environment in brain affecting conditions. *Front Immunol* **16**, 1711656 (2025). https://doi.org:10.3389/fimmu.2025.1711656

78 Sarode, G. *et al.* Cigarette smoking induces NLRP3 inflammasome activation in patients with atrial fibrillation. *Am J Physiol Heart Circ Physiol* **329**, H1287-H1295 (2025). https://doi.org:10.1152/ajpheart.00624.2025

79 Rumora, L. *et al.* Assessment of NLRP3 inflammasome activation in patients with chronic obstructive pulmonary disease before and after lung transplantation. *Immunol Res* **72**, 964-974 (2024). https://doi.org:10.1007/s12026-024-09497-2

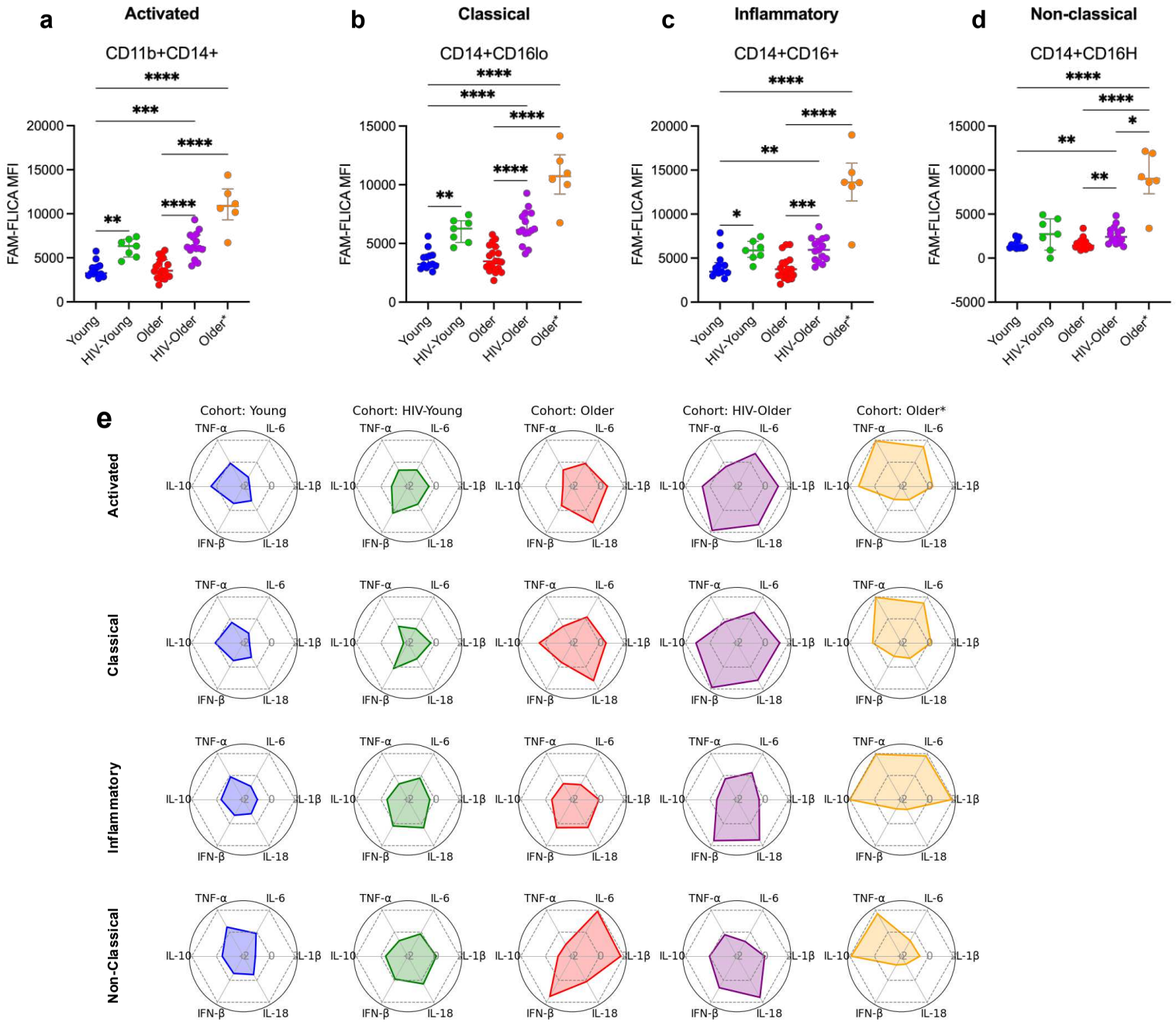
80 Zahid, A., Li, B., Kombe, A. J. K., Jin, T. & Tao, J. Pharmacological Inhibitors of the NLRP3 Inflammasome. *Front Immunol* **10**, 2538 (2019). https://doi.org:10.3389/fimmu.2019.02538

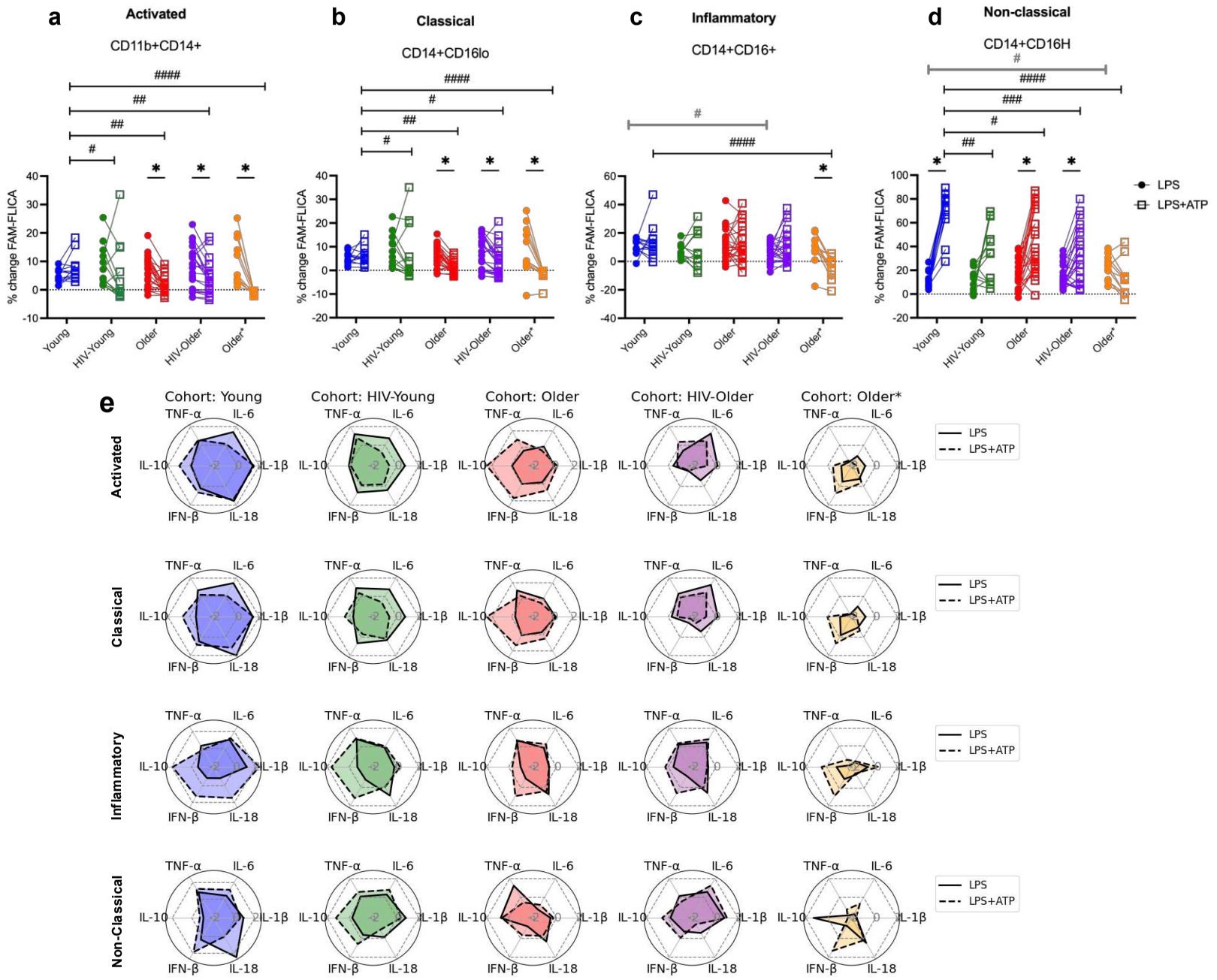
81 Puleo, A., Carroll, C., Maecker, H. T. & Gupta, R. Isolation of Peripheral Blood Mononuclear Cells Using Vacutainer® Cellular Preparation Tubes (CPTTM). *Bio-protocol* **7**, e2103-e2103 (2017). https://doi.org:10.21769/BIOPROTOC.2103

82 Martin, M. Cutadapt removes adapter sequences from high-throughput sequencing reads. *EMBnet.journal* **17**, 10-12 (2011). https://doi.org:10.14806/EJ.17.1.200

83 Andrews, S. *FastQC: A quality control tool for high throughput sequence data*, <https://www.bioinformatics.babraham.ac.uk/projects/fastqc/> (2010).

84 Dobin, A. *et al.* STAR: ultrafast universal RNA-seq aligner. *Bioinformatics* **29**, 15-21 (2013). https://doi.org:10.1093/BIOINFORMATICS/BTS635

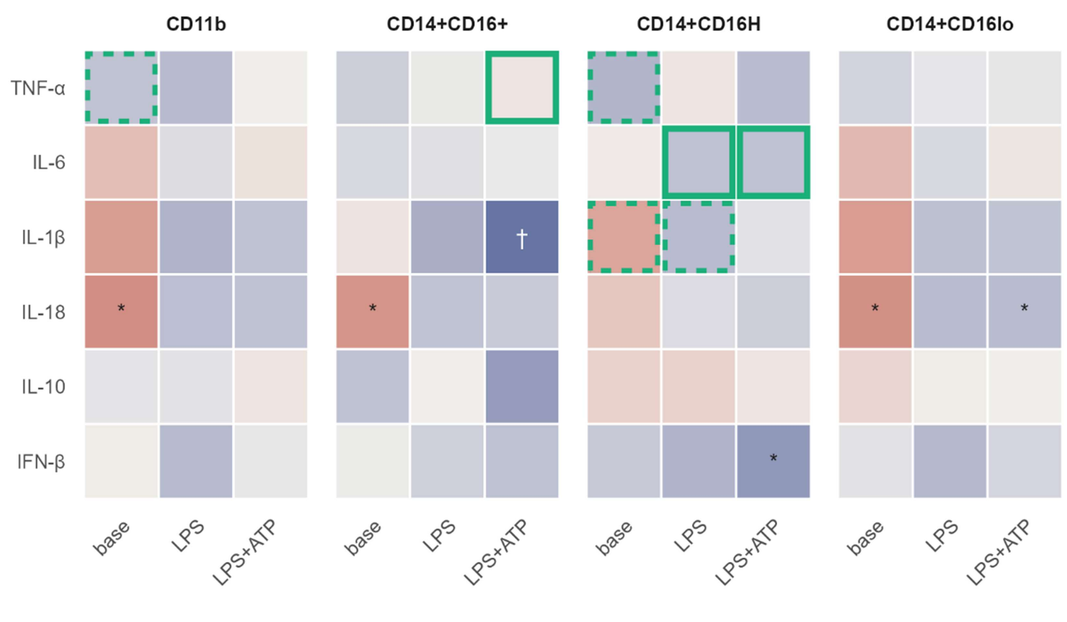

a
Activated
CD11b+CD14+
b
Classical
CD14+CD16lo
c
Inflammatory
CD14+CD16+
d
Non-classical
CD14+CD16H
FAM-FLICA MFI
Young
HIV-Young
Older
HIV-Older
Older*
e
Cohort: Young
Cohort: HIV-Young
Cohort: Older
Cohort: HIV-Older
Cohort: Older*
Activated
Classical
Inflammatory
Non-Classical
TNF-α
IL-6
IL-1β
IL-18
IFN-β
IL-10


a
Activated
CD11b+CD14+
b
Classical
CD14+CD16lo
c
Inflammatory
CD14+CD16+
d
Non-classical
CD14+CD16H
% change FAM-FLICA
Young
HIV-Young
Older
HIV-Older
Older*
LPS
LPS+ATP
e
Cohort: Young
Cohort: HIV-Young
Cohort: Older
Cohort: HIV-Older
Cohort: Older*
Activated
Classical
Inflammatory
Non-Classical
TNF-α
IL-6
IL-1β
IL-18
IFN-β
IL-10

Age and HIV effects on response_z

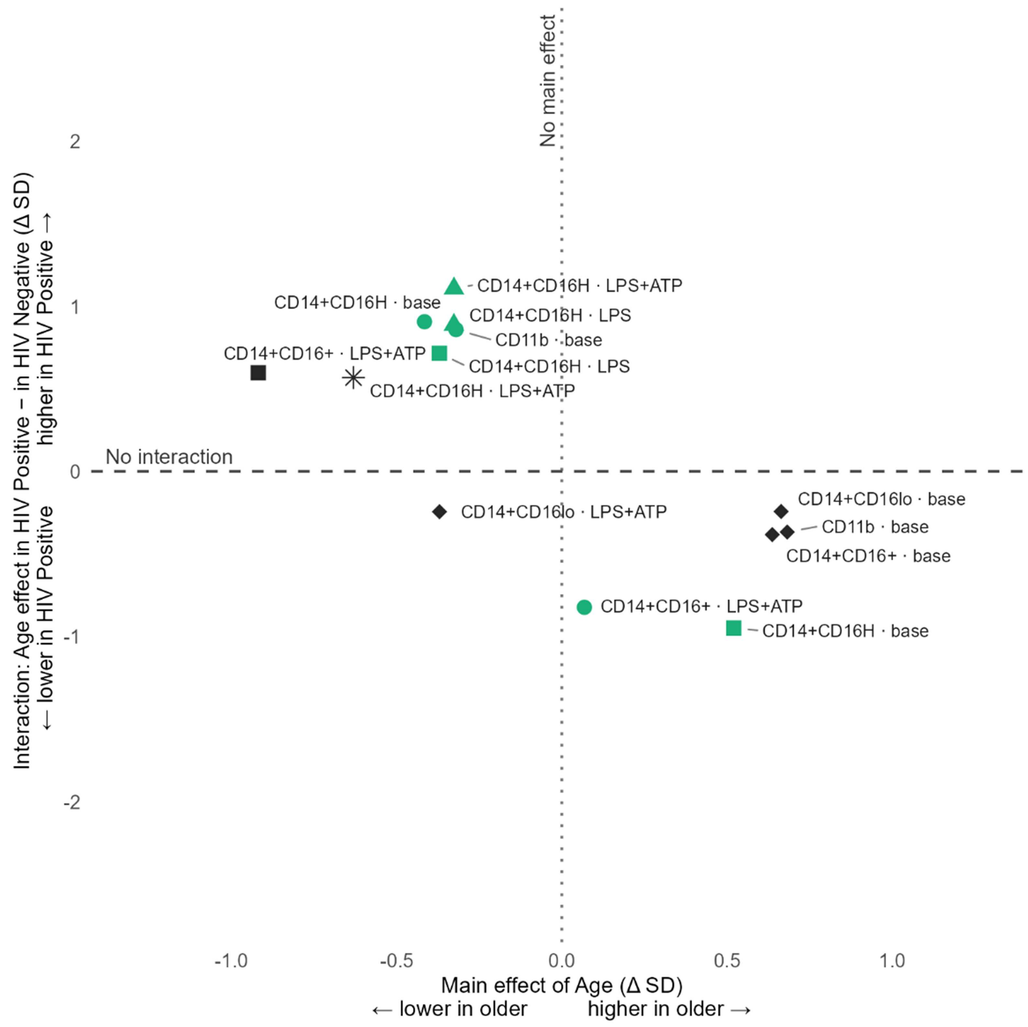
a

Age effect (older − younger)



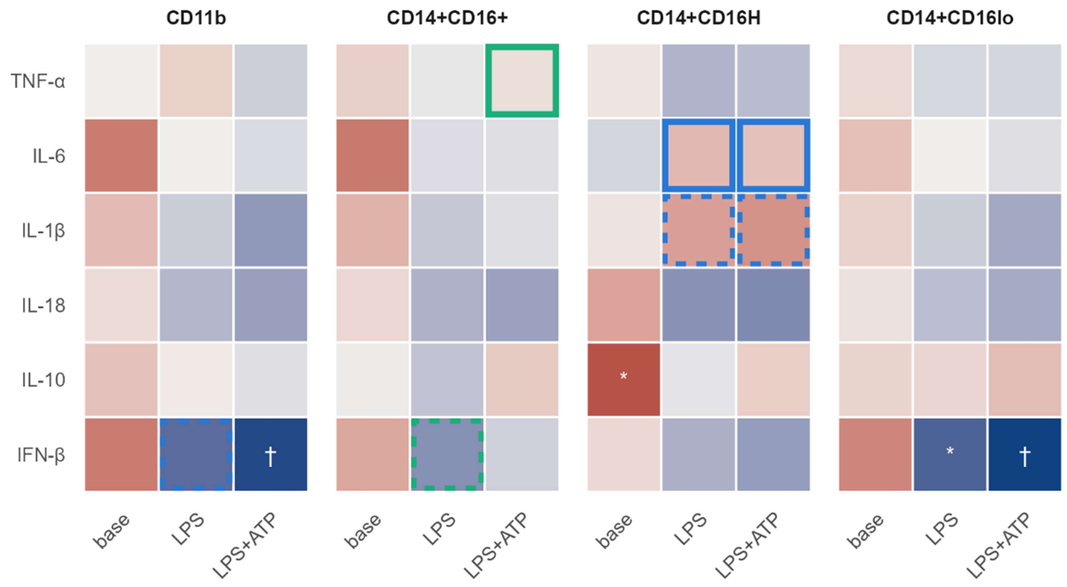
b

Age Effect (Older − younger), Main effect vs interaction



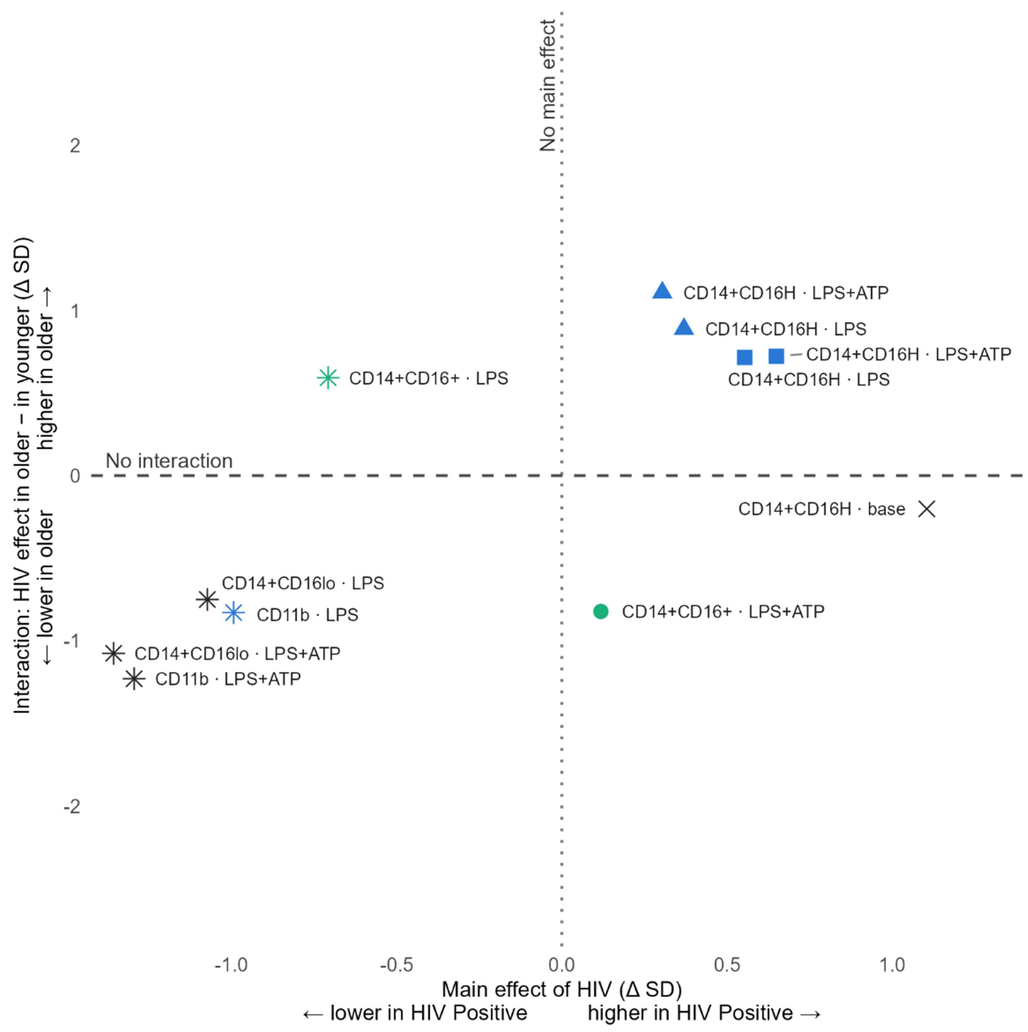
c

HIV effect (HIV Positive − HIV Negative)



d

HIV Effect (HIV Positive − HIV Negative), Main effect vs interaction



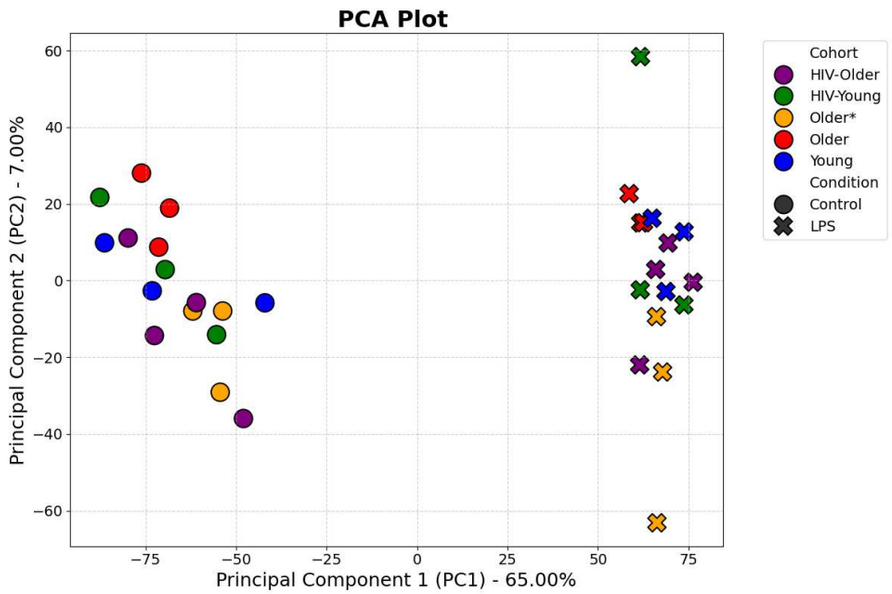
Main effect (Δ SD)
red: higher in older (a)
or HIV Positive (c)

-1.0 -0.5 0.0 0.5 1.0

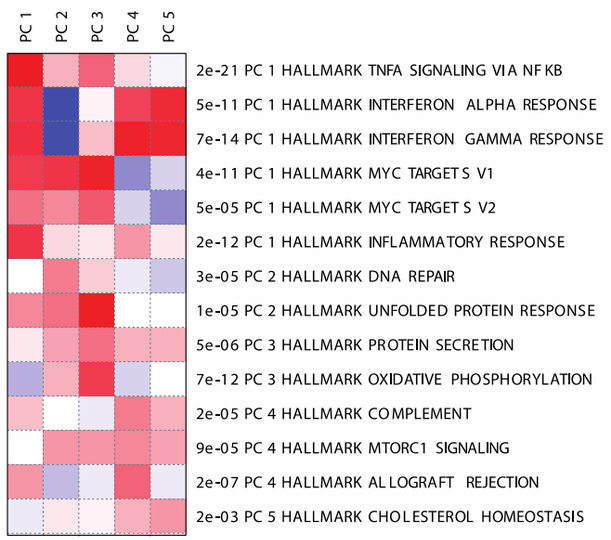
Marker: ● TNF-α ▲ IL-6 ■ IL-1β ◆ IL-18 × IL-10 ✳ IFN-β

Effect: ● Crossover ● Amplified ● Attenuated ● Main effect only

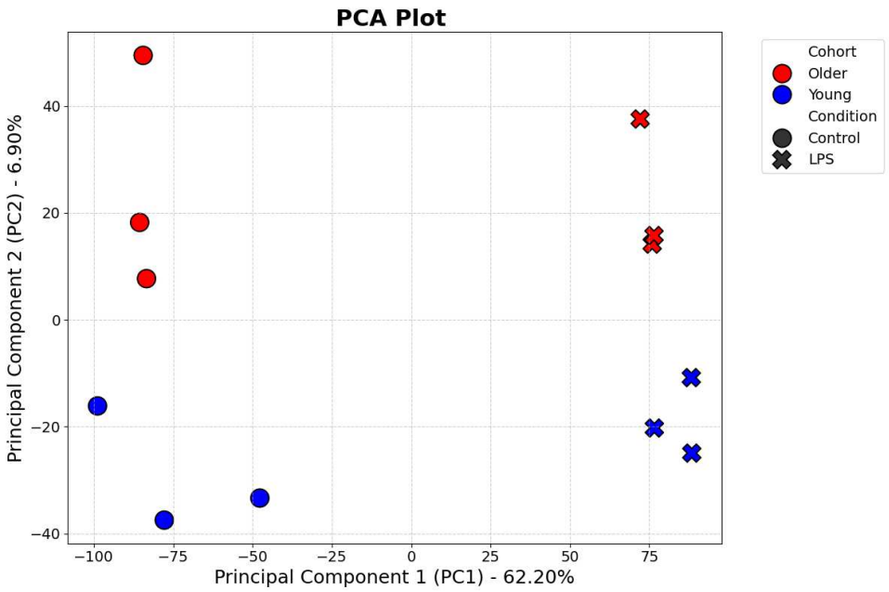
a


PCA Plot
Principal Component 2 (PC2) - 7.00%
Principal Component 1 (PC1) - 65.00%
60
40
20
0
−20
−40
−60
−75
−50
−25
0
25
50
75
Cohort
HIV-Older
HIV-Young
Older*
Older
Young
Condition
Control
LPS

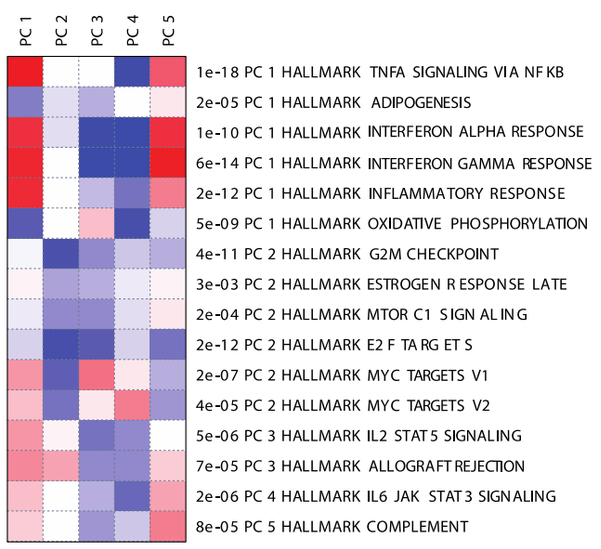
b


PC 1
PC 2
PC 3
PC 4
PC 5
2e-21 PC 1 HALLMARK TNFA SIGNALING VIA NFKB
5e-11 PC 1 HALLMARK INTERFERON ALPHA RESPONSE
7e-14 PC 1 HALLMARK INTERFERON GAMMA RESPONSE
4e-11 PC 1 HALLMARK MYC TARGETS V1
5e-05 PC 1 HALLMARK MYC TARGETS V2
2e-12 PC 1 HALLMARK INFLAMMATORY RESPONSE
3e-05 PC 2 HALLMARK DNA REPAIR
1e-05 PC 2 HALLMARK UNFOLDED PROTEIN RESPONSE
5e-06 PC 3 HALLMARK PROTEIN SECRETION
7e-12 PC 3 HALLMARK OXIDATIVE PHOSPHORYLATION
2e-05 PC 4 HALLMARK COMPLEMENT
9e-05 PC 4 HALLMARK MTORC1 SIGNALING
2e-07 PC 4 HALLMARK ALLOGRAFT REJECTION
2e-03 PC 5 HALLMARK CHOLESTEROL HOMEOSTASIS

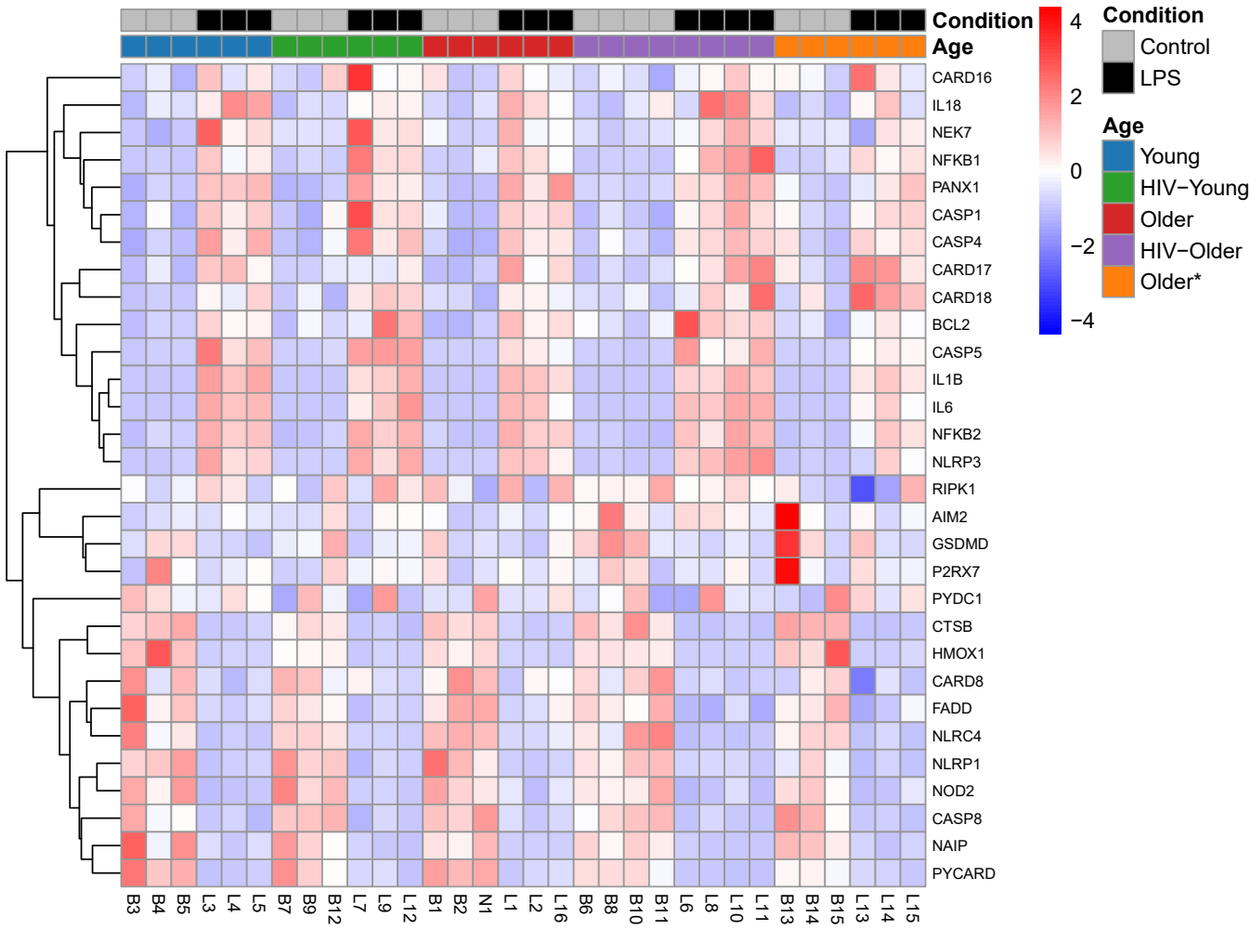
c


PCA Plot
Principal Component 2 (PC2) - 6.90%
Principal Component 1 (PC1) - 62.20%
40
20
0
−20
−40
−100
−75
−50
−25
0
25
50
75
Cohort
Older
Young
Condition
Control
LPS

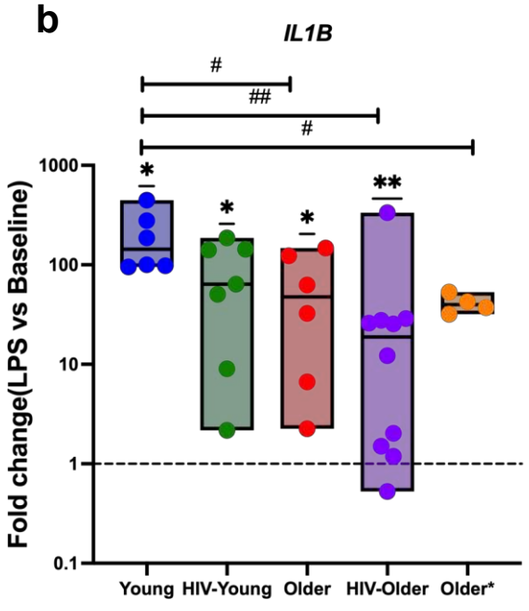
d


PC 1
PC 2
PC 3
PC 4
PC 5
1e-18 PC 1 HALLMARK TNFA SIGNALING VIA NFKB
2e-05 PC 1 HALLMARK ADIPOGENESIS
1e-10 PC 1 HALLMARK INTERFERON ALPHA RESPONSE
6e-14 PC 1 HALLMARK INTERFERON GAMMA RESPONSE
2e-12 PC 1 HALLMARK INFLAMMATORY RESPONSE
5e-09 PC 1 HALLMARK OXIDATIVE PHOSPHORYLATION
4e-11 PC 2 HALLMARK G2M CHECKPOINT
3e-03 PC 2 HALLMARK ESTROGEN RESPONSE LATE
2e-04 PC 2 HALLMARK MTORC1 SIGNALING
2e-12 PC 2 HALLMARK E2F TARGETS
2e-07 PC 2 HALLMARK MYC TARGETS V1
4e-05 PC 2 HALLMARK MYC TARGETS V2
5e-06 PC 3 HALLMARK IL2 STAT5 SIGNALING
7e-05 PC 3 HALLMARK ALLOGRAFT REJECTION
2e-06 PC 4 HALLMARK IL6 JAK STAT3 SIGNALING
8e-05 PC 5 HALLMARK COMPLEMENT

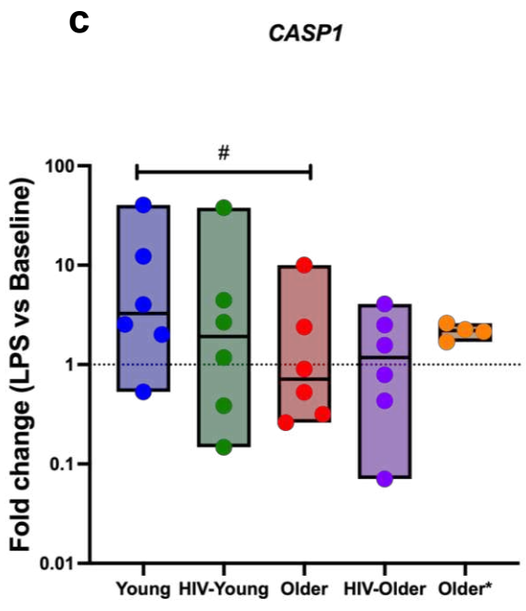
a


Condition
Age
CARD16
IL18
NEK7
NFKB1
PANX1
CASP1
CASP4
CARD17
CARD18
BCL2
CASP5
IL1B
IL6
NFKB2
NLRP3
RIPK1
AIM2
GSDMD
P2RX7
PYDC1
CTSB
HMOX1
CARD8
FADD
NLRC4
NLRP1
NOD2
CASP8
NAIP
PYCARD
B3 B4 B5 L3 L4 L5 B7 B9 B12 L7 L9 L12 B1 B2 N1 L1 L2 L16 B6 B8 B10 B11 L6 L8 L10 L11 B13 B14 B15 L13 L14 L15
4
2
0
−2
−4
Condition
Control
LPS
Age
Young
HIV−Young
Older
HIV−Older
Older*

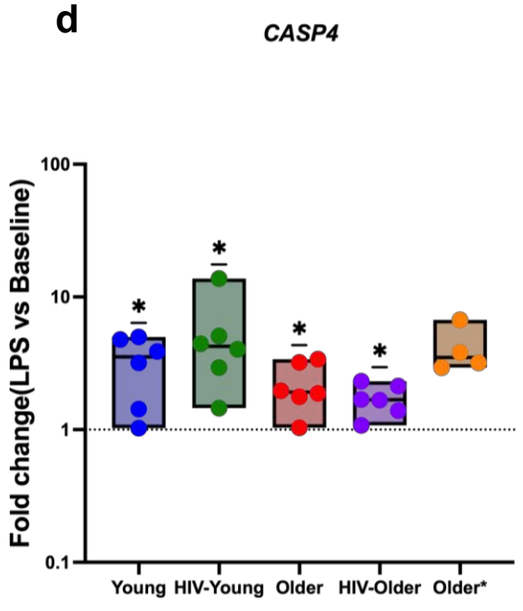
b


IL1B
Fold change(LPS vs Baseline)
1000
100
10
1
0.1
#
##
#
*
*
*
**
Young HIV-Young Older HIV-Older Older*

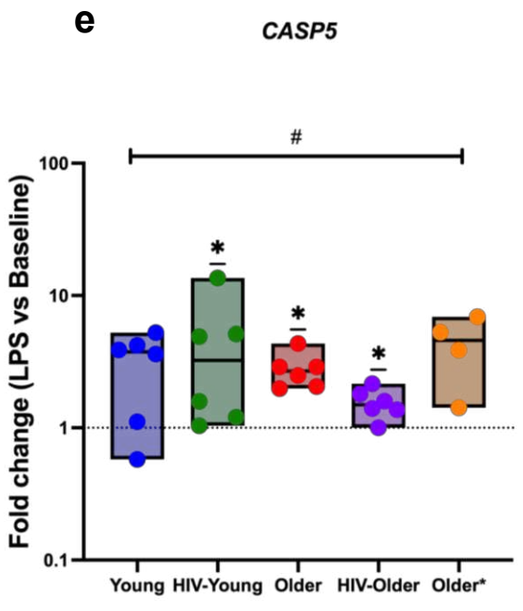
c

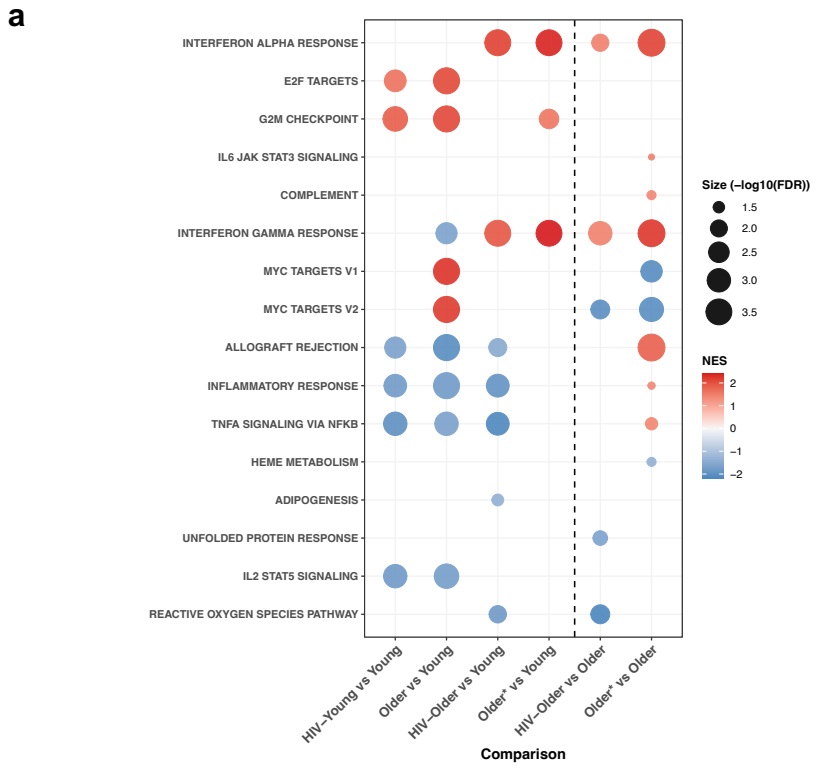

CASP1
Fold change (LPS vs Baseline)
100
10
1
0.1
0.01
#
Young HIV-Young Older HIV-Older Older*

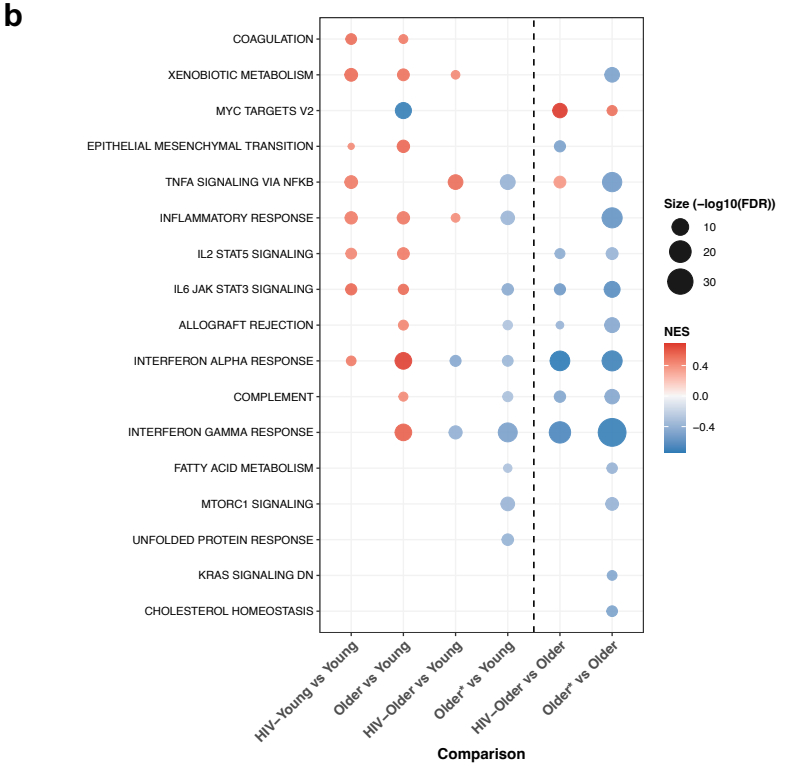
d

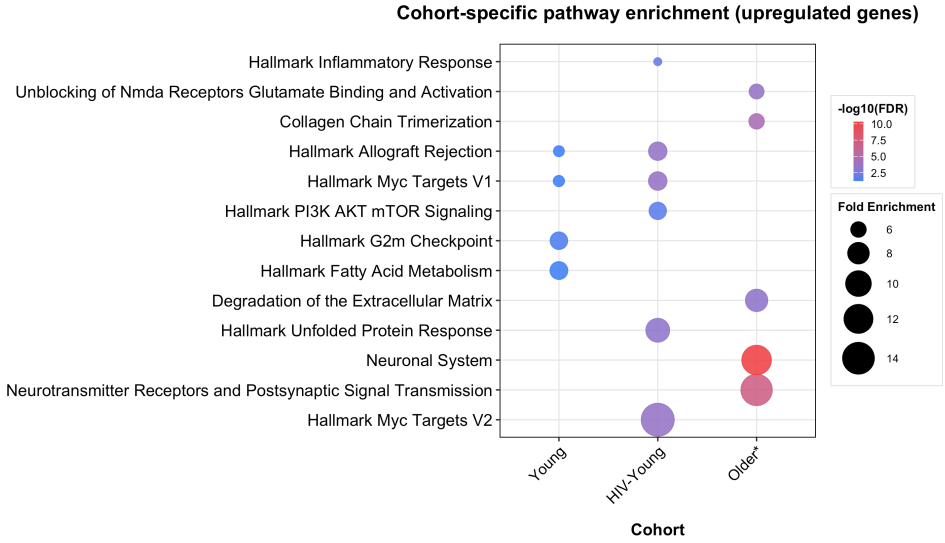

CASP4
Fold change(LPS vs Baseline)
100
10
1
0.1
*
*
*
*
Young HIV-Young Older HIV-Older Older*

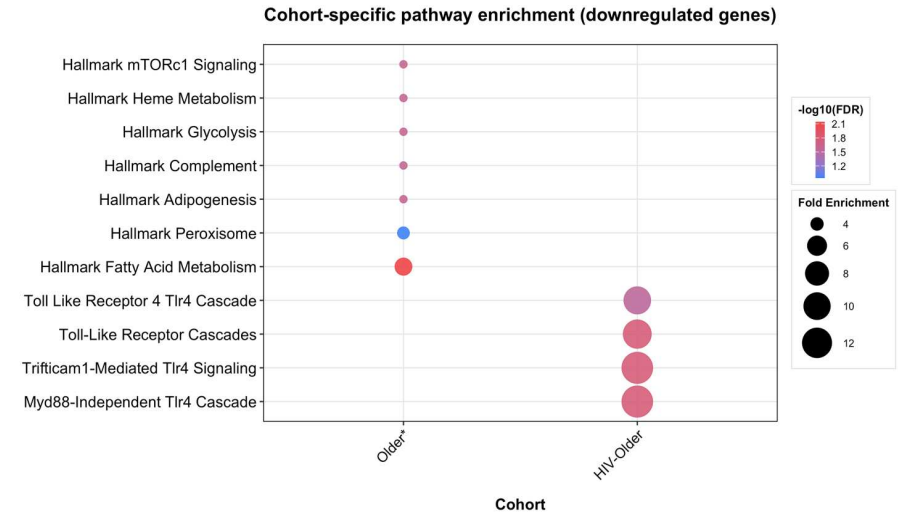
e

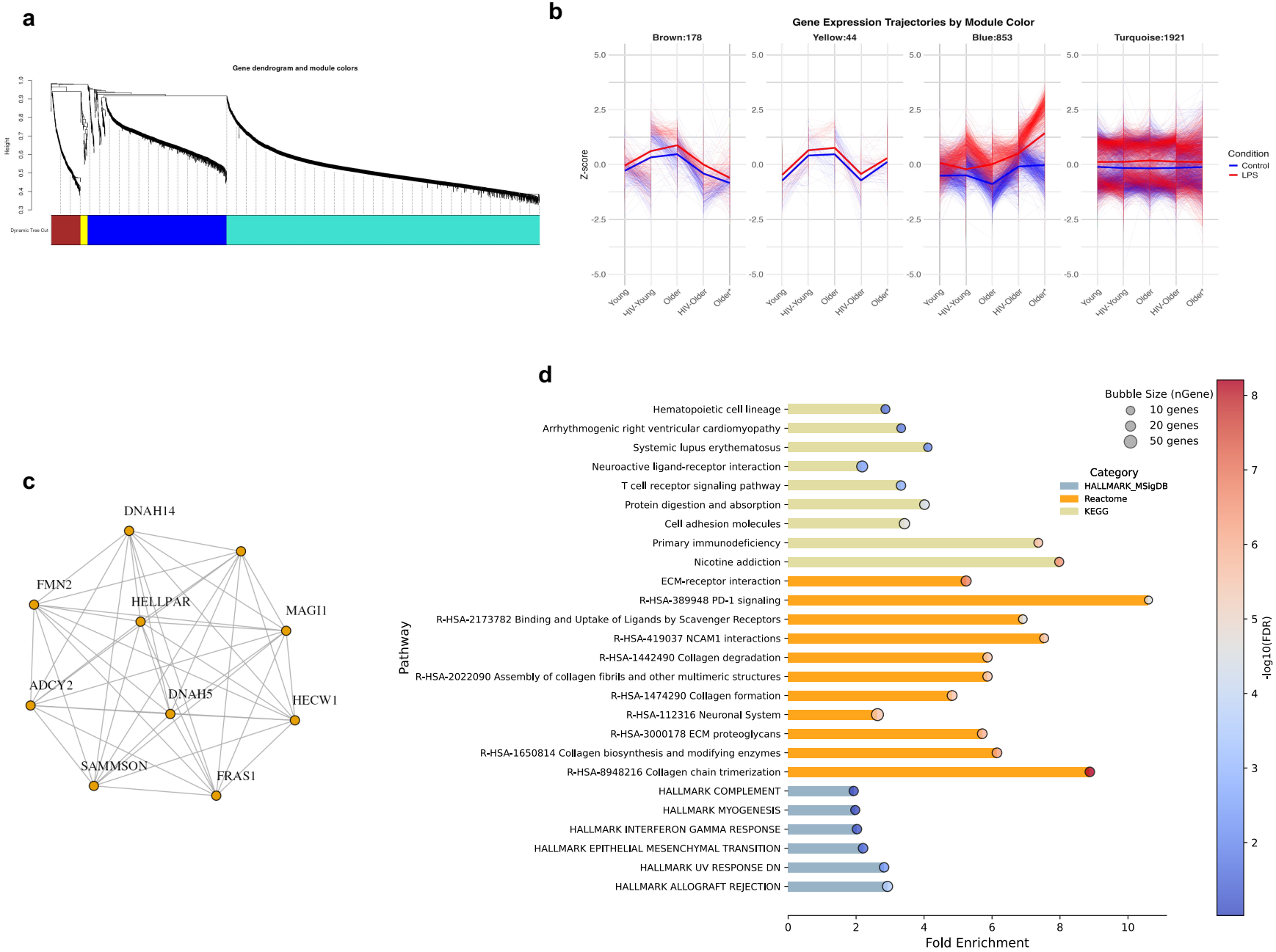

CASP5
Fold change (LPS vs Baseline)
100
10
1
0.1
#
*
*
*
Young HIV-Young Older HIV-Older Older*


a
INTERFERON ALPHA RESPONSE
E2F TARGETS
G2M CHECKPOINT
IL6 JAK STAT3 SIGNALING
COMPLEMENT
INTERFERON GAMMA RESPONSE
MYC TARGETS V1
MYC TARGETS V2
ALLOGRAFT REJECTION
INFLAMMATORY RESPONSE
TNFA SIGNALING VIA NFKB
HEME METABOLISM
ADIPOGENESIS
UNFOLDED PROTEIN RESPONSE
IL2 STAT5 SIGNALING
REACTIVE OXYGEN SPECIES PATHWAY
HIV−Young vs Young
Older vs Young
HIV−Older vs Young
Older* vs Young
HIV−Older vs Older
Older* vs Older
Comparison
Size (−log10(FDR))
1.5
2.0
2.5
3.0
3.5
NES
2
1
0
−1
−2


b
COAGULATION
XENOBIOTIC METABOLISM
MYC TARGETS V2
EPITHELIAL MESENCHYMAL TRANSITION
TNFA SIGNALING VIA NFKB
INFLAMMATORY RESPONSE
IL2 STAT5 SIGNALING
IL6 JAK STAT3 SIGNALING
ALLOGRAFT REJECTION
INTERFERON ALPHA RESPONSE
COMPLEMENT
INTERFERON GAMMA RESPONSE
FATTY ACID METABOLISM
MTORC1 SIGNALING
UNFOLDED PROTEIN RESPONSE
KRAS SIGNALING DN
CHOLESTEROL HOMEOSTASIS
HIV−Young vs Young
Older vs Young
HIV−Older vs Young
Older* vs Young
HIV−Older vs Older
Older* vs Older
Comparison
Size (−log10(FDR))
10
20
30
NES
0.4
0.0
−0.4


c
Cohort-specific pathway enrichment (upregulated genes)
Hallmark Inflammatory Response
Unblocking of Nmda Receptors Glutamate Binding and Activation
Collagen Chain Trimerization
Hallmark Allograft Rejection
Hallmark Myc Targets V1
Hallmark PI3K AKT mTOR Signaling
Hallmark G2m Checkpoint
Hallmark Fatty Acid Metabolism
Degradation of the Extracellular Matrix
Hallmark Unfolded Protein Response
Neuronal System
Neurotransmitter Receptors and Postsynaptic Signal Transmission
Hallmark Myc Targets V2
Young
HIV-Young
Older*
Cohort
-log10(FDR)
10.0
7.5
5.0
2.5
Fold Enrichment
6
8
10
12
14


d
Cohort-specific pathway enrichment (downregulated genes)
Hallmark mTORc1 Signaling
Hallmark Heme Metabolism
Hallmark Glycolysis
Hallmark Complement
Hallmark Adipogenesis
Hallmark Peroxisome
Hallmark Fatty Acid Metabolism
Toll Like Receptor 4 Tlr4 Cascade
Toll-Like Receptor Cascades
Trifticam1-Mediated Tlr4 Signaling
Myd88-Independent Tlr4 Cascade
Older*
HIV-Older
Cohort
-log10(FDR)
2.1
1.8
1.5
1.2
Fold Enrichment
4
6
8
10
12


a
Gene dendrogram and module colors
Height
Dynamic Tree Cut
b
Gene Expression Trajectories by Module Color
Brown:178
Yellow:44
Blue:853
Turquoise:1921
Z-score
Young
HIV-Young
Older
HIV-Older
Older*
Condition
Control
LPS
c
DNAH14
FMN2
HELLPAR
MAGI1
ADCY2
DNAH5
HECW1
SAMMSON
FRAS1
d
Bubble Size (nGene)
10 genes
20 genes
50 genes
Category
HALLMARK_MSigDB
Reactome
KEGG
Pathway
Hematopoietic cell lineage
Arrhythmogenic right ventricular cardiomyopathy
Systemic lupus erythematosus
Neuroactive ligand-receptor interaction
T cell receptor signaling pathway
Protein digestion and absorption
Cell adhesion molecules
Primary immunodeficiency
Nicotine addiction
ECM-receptor interaction
R-HSA-389948 PD-1 signaling
R-HSA-2173782 Binding and Uptake of Ligands by Scavenger Receptors
R-HSA-419037 NCAM1 interactions
R-HSA-1442490 Collagen degradation
R-HSA-2022090 Assembly of collagen fibrils and other multimeric structures
R-HSA-1474290 Collagen formation
R-HSA-112316 Neuronal System
R-HSA-3000178 ECM proteoglycans
R-HSA-1650814 Collagen biosynthesis and modifying enzymes
R-HSA-8948216 Collagen chain trimerization
HALLMARK COMPLEMENT
HALLMARK MYOGENESIS
HALLMARK INTERFERON GAMMA RESPONSE
HALLMARK EPITHELIAL MESENCHYMAL TRANSITION
HALLMARK UV RESPONSE DN
HALLMARK ALLOGRAFT REJECTION
Fold Enrichment
-log10(FDR)

Characteristics	N (150)	HIV-negative Young N = 53	HIV-positive Young N = 27	HIV-negative Older N = 30	HIV-positive Older N = 29	Older* N = 11	p-value
Age †	147	36 (13)	39 (13)	74 (6)	69 (4)	68 (2)	<0.001
Sex	129						0.006
Male		13 (30%)	16 (67%)	11 (44%)	15 (60%)	2 (18%)	
Female		31 (70%)	8 (33%)	14 (56%)	10 (40%)	9 (82%)	
Race/ethnicity (Non-White or Hispanic)	129	20 (45%)	23 (96%)	1 (4.0%)	23 (92%)	6 (55%)	<0.001
Race	128						
White		27 (63%)	4 (17%)	24 (96%)	2 (8.0%)	6 (55%)	
Black or African-American		7 (16%)	18 (75%)	0 (0%)	22 (88%)	5 (45%)	
Asian		3 (7.0%)	0 (0%)	0 (0%)	0 (0%)	0 (0%)	
American Indian or Alaskan Native		0 (0%)	0 (0%)	0 (0%)	0 (0%)	0 (0%)	
Native Hawaiian or Pacific Islander		0 (0%)	0 (0%)	0 (0%)	0 (0%)	0 (0%)	
More than 1 race		0 (0%)	0 (0%)	0 (0%)	0 (0%)	0 (0%)	
Refused		1 (2.3%)	2 (8.3%)	1 (4.0%)	1 (4.0%)	0 (0%)	
Other or Unknown		5 (12%)	0 (0%)	0 (0%)	0 (0%)	0 (0%)	
Hispanic	129	10 (23%)	3 (13%)	0 (0%)	0 (0%)	1 (9.1%)	0.007
Approximate years infected†	49	NA (NA)	13 (10)	NA (NA)	22 (9)	NA (NA)	0.002
HIV Viral load†	36	NA (NA)	11 (16)	NA (NA)	99 (388)	NA (NA)	0.7
HIV Viral load ≥ 100	36	0 (NA%)	0 (0%)	0 (NA%)	1 (5.3%)	0 (NA%)	>0.9
CD4 count (CD3 + CD4 + Abs count)†	53	NA (NA)	781 (267)	NA (NA)	712 (225)	NA (NA)	0.11
CD4 count < 200	53	0 (NA%)	25 (93%)	0 (NA%)	26 (100%)	0 (NA%)	0.5
CD4 count % (CD3 +CD4) †	53	NA (NA)	37 (11)	NA (NA)	37 (10)	NA (NA)	>0.9
CD4/CD8 Ratio†	53	NA (NA)	1.33 (0.63)	NA (NA)	1.41 (0.66)	NA (NA)	>0.9
Prior fungal infection	104	1 (4.0%)	3 (11%)	1 (6.3%)	7 (28%)	0 (0%)	0.073
Prior positive PPD	105	0 (0%)	2 (7.4%)	0 (0%)	11 (42%)	1 (9.1%)	<0.001
History of tuberculosis	112	0 (0%)	1 (3.7%)	0 (0%)	4 (15%)	0 (0%)	0.053
Irregular heart rhythm (Arrhythmia)	150	0 (0%)	0 (0%)	10 (33%)	6 (21%)	0 (0%)	<0.001
Asplenia	150	0 (0%)	0 (0%)	0 (0%)	0 (0%)	0 (0%)	>0.9
Asthma	150	7 (13%)	9 (33%)	6 (20%)	7 (24%)	4 (36%)	0.2
Autoimmune/Inflammatory Disease	149	1 (1.9%)	3 (11%)	2 (6.9%)	1 (3.4%)	2 (18%)	0.12
Coronary Artery Disease	150	0 (0%)	0 (0%)	5 (17%)	8 (28%)	0 (0%)	<0.001
Heart failure	145	0 (0%)	2 (7.4%)	0 (0%)	2 (8.3%)	0 (0%)	0.074
Colitis / IBS	145	1 (1.9%)	0 (0%)	2 (6.7%)	0 (0%)	0 (0%)	0.5
Chronic pulmonary disease / Emphysema	145	1 (1.9%)	0 (0%)	4 (13%)	3 (13%)	4 (36%)	0.001
Depression	150	10 (19%)	18 (67%)	6 (20%)	13 (45%)	0 (0%)	<0.001
Diabetes	150	1 (1.9%)	0 (0%)	5 (17%)	8 (28%)	3 (27%)	<0.001
GERD	150	7 (13%)	8 (30%)	11 (37%)	6 (21%)	3 (27%)	0.12
On ART	55	0 (NA%)	25 (93%)	0 (0%)	25 (96%)	0 (NA%)	0.007
Hypertension	150	9 (17%)	18 (67%)	23 (77%)	23 (79%)	9 (82%)	<0.001
High Cholesterol	150	7 (13%)	8 (30%)	23 (77%)	20 (69%)	8 (73%)	<0.001
Kidney disease	150	2 (3.8%)	1 (3.7%)	2 (6.7%)	10 (34%)	0 (0%)	<0.001
Liver disease	150	3 (5.7%)	2 (7.4%)	0 (0%)	5 (17%)	1 (9.1%)	0.11
Metabolic syndrome	140	5 (10%)	3 (11%)	7 (25%)	6 (23%)	4 (36%)	0.14
Heart Attack	150	1 (1.9%)	0 (0%)	0 (0%)	1 (3.4%)	0 (0%)	0.9
Osteoarthritis	150	1 (1.9%)	6 (22%)	14 (47%)	10 (34%)	1 (9.1%)	<0.001

Peripheral vascular disease	150	1 (1.9%)	0 (0%)	3 (10%)	6 (21%)	0 (0%)	0.008
Obstructive sleep apnea	150	6 (11%)	4 (15%)	5 (17%)	4 (14%)	2 (18%)	>0.9
Thyroid disease	150	1 (1.9%)	2 (7.4%)	13 (43%)	0 (0%)	3 (27%)	<0.001
Valvular Disease	150	0 (0%)	0 (0%)	4 (13%)	6 (21%)	0 (0%)	<0.001
Substance drug abuse	132	16 (35%)	5 (19%)	0 (0%)	7 (32%)	0 (0%)	<0.001
Past alcohol abuse	134	4 (8.7%)	4 (15%)	0 (0%)	10 (42%)	1 (9.1%)	<0.001
Current smoker	134	2 (4.3%)	5 (19%)	4 (15%)	9 (39%)	5 (45%)	<0.001
Past smoker	135	7 (15%)	6 (22%)	10 (37%)	11 (46%)	4 (36%)	0.045
Chronic condition count†	150	1.21 (1.68)	3.11 (1.80)	4.83 (2.56)	5.00 (3.40)	4.00 (1.79)	<0.001
Chronic condition count w/ smoking, illicit drugs, alcohol abuse †	150	1.75 (2.08)	3.85 (2.21)	5.30 (2.69)	6.28 (4.03)	4.91 (1.97)	<0.001
BMI†	140	30 (10)	30 (6)	28 (7)	26 (3)	28 (7)	0.5
BMI level	139						
BMI 25-29.99 kg/m2		17 (36%)	6 (22%)	9 (32%)	17 (65%)	3 (27%)	
BMI 18.5-24.99 kg/m2		12 (26%)	8 (30%)	13 (46%)	6 (23%)	5 (45%)	
BMI >=30 kg/m2		18 (38%)	13 (48%)	6 (21%)	3 (12%)	3 (27%)	

Table 1: Overall Characteristics and Co-morbid Conditions of All Participants.
Caption: Categorical variables are given as N (%) and tested using a Fisher's exact test. † Continuous variables are given as Mean (SD) tested using a Kruskal-Wallis rank sum test. The full categorization of the race variable was not assessed due to sparseness.

Variable	HIV-negative Young N = 14	HIV-negative Older N = 10	HIV-positive Young N = 9	HIV-positive Older N = 16	p-value
Sex					0.194
Female	8 (57.1%)	4 (40.0%)	1 (11.1%)	7 (43.8%)	
Male	6 (42.9%)	6 (60.0%)	8 (88.9%)	9 (56.3%)	
Race/Ethnicity					<0.001
White and non-Hispanic	10 (71.4%)	9 (90.0%)	1 (11.1%)	1 (6.3%)	
Non-White or Hispanic	4 (28.6%)	1 (10.0%)	8 (88.9%)	15 (93.8%)	

Table 2: Sex and Race Variables Across Cohorts

Caption: N (%) of characteristics in the factorial analysis (age x hiv) cohorts. Fischer's exact test was used to test differences. The Older* cohort is not included in this table or analysis.

Variable	N	HIV-negative Older N = 10	HIV-positive Older N = 16	Older* N=11	p-value
Sex	37				0.094
Female		4 (40.0%)	7 (43.8%)	9 (81.8%)	
Male		6 (60.0%)	9 (56.3%)	2 (18.2%)	
Race/Ethnicity	37				<0.001
White and non-Hispanic		9 (90.0%)	1 (6.3%)	5 (45.5%)	
Non-White or Hispanic		1 (10.0%)	15 (93.8%)	6 (54.5%)	
Count of chronic conditions	37	5.20 (1.99)	5.44 (3.97)	4.91 (1.97)	0.905*
Behavioral cluster	37	4 (40.0%)	10 (62.5%)	8 (72.7%)	0.361
Cardiovascular cluster	37	10 (100.0%)	12 (75.0%)	9 (81.8%)	0.285
Metabolic Cluster	37	9 (90.0%)	13 (81.3%)	8 (72.7%)	0.768
Pulmonary cluster	37	3 (30.0%)	4 (25.0%)	7 (63.6%)	0.134
Inflammatory cluster	37	9 (90.0%)	4 (25.0%)	6 (54.5%)	0.006
Organ failure cluster	37	0 (0.0%)	6 (37.5%)	1 (9.1%)	0.05

Table 3: Comparison of Older Cohorts.

Caption: N (%) or Mean (SD) for characteristics in the analysis of the older cohorts. Fischer's exact test was used for dichotomous variables and a one-way test of means for the count of chronic conditions (*). Condition clusters consisted of: behavioral cluster (smoking, alcohol abuse, and polysubstance use), cardiovascular cluster (hypertension, CAD, MI, CHF, PVD, arrythmias, valvular disease), metabolic cluster (BMI > 30, diabetes, high cholesterol), pulmonary cluster (asthma, COPD, sleep apnea), inflammatory cluster, (autoimmune disease, colitis, thyroid disease, osteoarthritis) and organ failure cluster (kidney disease, liver disease)

CAD = Coronary Artery Disease, MI= Myocardial Infarction, CHF= Congestive Heart Failure, PVD = Peripheral vascular disease, COPD= Chronic Obstructive Pulmonary Disease. This table only examines subjects studied in flow cytometry studies.

Characteristic	Other Older Cohorts N = 26	Older* N = 11	p-value
COPD	**1 (3.8%)**	**4 (36%)**	**0.021**
Osteoarthritis	**11 (42%)**	**1 (9.1%)**	**0.064**
Smoking	**4 (15%)**	**5 (45%)**	**0.091**
Arrythmias	6 (23%)	0 (0%)	0.2
Depression	6 (23%)	0 (0%)	0.2
Kidney disease	6 (23%)	0 (0%)	0.2
Asthma	4 (15%)	4 (36%)	0.2
CAD	4 (15%)	0 (0%)	0.3
Thyroid disease	4 (15%)	3 (27%)	0.4
Metabolic Syndrome	6 (23%)	4 (36%)	0.4
Valvular heart disease	3 (12%)	0 (0%)	0.5
Autoimmune disease	3 (12%)	2 (18%)	0.6
Obstructive Sleep Apnea	3 (12%)	2 (18%)	0.6
GERD	10 (38%)	3 (27%)	0.7
Congestive Heart Failure	1 (3.8%)	0 (0%)	>0.9
Colitis	2 (7.7%)	0 (0%)	>0.9
Diabetes	6 (23%)	3 (27%)	>0.9
On ART	12 (92%)	0 (NA%)	>0.9
HTN	20 (77%)	9 (82%)	>0.9
HLD	19 (73%)	8 (73%)	>0.9
Liver disease	2 (7.7%)	1 (9.1%)	>0.9
Myocardial Infarction	1 (3.8%)	0 (0%)	>0.9
Peripheral vascular disease	2 (7.7%)	0 (0%)	>0.9
Substance Abuse	2 (7.7%)	0 (0%)	>0.9
Alcohol abuse	4 (15%)	1 (9.1%)	>0.9
Smoking in past	9 (35%)	4 (36%)	>0.9

Table 4: Older * versus other Older Cohorts

Caption: N (%) for individual chronic conditions in the analysis of the older cohorts, Older* vs the non-Older* (HIV-positive Older and HIV-negative Older). Differences were assessed with Fisher's exact test. A p-value cut-off of .2 was used for inclusion in the attenuation analysis. This table only examines subjects studied in flow cytometry studies.

Supplementary Files

This is a list of supplementary files associated with this preprint. Click to download.

- SupplementaryFigures.pdf